Mon. Not. R. Astron. Soc. **347,** 1–16 (2004)

Extremely red galaxies: dust attenuation and classification

D. Pierini,[1]★ C. Maraston,[1] R. Bender[1,2] and A. N. Witt[3]

[1]*Max-Planck-Institut für extraterrestrische Physik, Giessenbachstr, D-85748 Garching, Germany*
[2]*Universitäts-Sternwarte München, Scheinerstr. 1, D-81679 München, Germany*
[3]*Ritter Astrophysical Research Centre, The University of Toledo, Toledo, OH 43606, USA*

Accepted 2003 September 3. Received 2003 August 25; in original form 2002 December 20

ABSTRACT

We re-address the classification criterion for extremely red galaxies (ERGs) of Pozzetti & Mannucci, which aims to separate, in the $I_c - K$ (or $R_c - K$) versus $J - K$ colour–colour diagram, passively evolving, old ($\geqslant$1 Gyr) stellar populations in a dust-free environment, associated with ellipticals (Es), from dusty starburst galaxies (DSGs), both at $1 < z < 2$. We explore a category of objects not considered previously, i.e. galaxies forming *in this redshift range* on a short (0.1 Gyr) time-scale and also observed in their early, dusty post-starburst phase. We also investigate the impact of structure of the dusty medium and the amount of dust on the observed optical/near-infrared (near-IR) colours of high-z DSGs/dusty post-starburst galaxies (DPSGs), through multiple-scattering radiative transfer calculations for a dust/stars configuration and an extinction function calibrated with nearby dusty starbursts. As a main result, we find that DPSGs, with ages between 0.2 and 1 Gyr, at $1.3 < z < 2$ mix with Es at $1 < z < 2$ for a large range in the amount of dust. This 'intrusion' is a source of concern for the present two-colour classification of ERGs. On the other hand, we confirm, in agreement with Pozzetti & Mannucci, that DSGs are well separated from Es, both at $1 < z < 2$, in the $I_c - K$ versus $J - K$ colour–colour diagram, whatever the structure (two-phase clumpy or homogeneous) of their dusty medium and the amount of dust. This result holds under the new hypothesis of high-z Es being as dusty as nearby ones. Thus the interpretation of the optical/near-IR colours of high-z Es may suffer from a multiple degeneracy among age, metallicity, dust and redshift. We also find that DPSGs at $z \sim 1$ mix with DSGs at $1 < z < 2$, as a function of the amount of dust and the structure of the dusty medium. All of these results help to explain the complexity of the ERG classification that has emerged from recent surveys. Model DSGs/DPSGs with $K < 20.5$ and selected as ERGs on the basis of their observed optical/near-IR colours span a large range in absorption efficiency and/or intrinsic ultraviolet-to-optical luminosity ratio. Consequently, the total emission from dust in the rest-frame mid-IR–(sub)millimetre ranges from $\sim 10^{10}$ to $\sim 5.6 \times 10^{12}$ $L_\odot$ for DPSGs to DSGs. This large dynamic range is consistent with estimates made from submillimetre observations of bright ($K < 19.5$–20) ERGs. Finally, we show that ERG samples are biased towards a lower fraction either of DSGs/DPSGs at $1.3 < z < 2$ or of DSGs/DPSGs at $z \sim 1$, when selection is made via either the $R_c - K \geqslant 5.3$ or the $I_c - K \geqslant 4$ colour criterion.

Key words: radiative transfer – dust, extinction – galaxies: elliptical and lenticular, cD – galaxies: high-redshift – galaxies: starburst.

1 INTRODUCTION

The extremely red objects (EROs), originally discovered in the K-band survey of Elston, Rieke & Rieke (1988), have become more and more present in deep near-infrared (near-IR) and optical surveys (see Yan & Thompson 2003 for a review). Operationally defined in terms of the observed optical/near-IR colours (e.g. $R_c - K \geqslant 5.3$ or $I_c - K \geqslant 4$), significantly different from those of typical field objects, EROs may nevertheless comprise an assorted mix of Galactic and extragalactic objects. We focus on the extremely red galaxies (ERGs), which account for the bulk of the observed EROs. For the optically selected ERGs, the contamination from active galactic nuclei (AGN) is less than 15 per cent (Alexander et al. 2002; Brusa

★E-mail: dpierini@mpe.mpg.de

et al. 2002; Smail et al. 2002), even though obscured, Compton-thin AGN, partly associated with dusty starbursts having large star formation rates (SFRs), most probably dominate X-ray-selected ERG samples (Stevens et al. 2003).

ERGs still lack an uncontroversial classification because their very red colours can be reproduced by at least two very different sets of spectral energy distributions (SEDs) not associated with an AGN: those expected for passively evolving, old ($\geqslant$1 Gyr) stellar populations in a dust-free environment, associated with ellipticals, and those expected for dusty starburst galaxies (DSGs), both at high redshift ($z > 1$). Indeed, it emerges that half or more of the entire ERG sample in the literature contains ellipticals (Moriondo, Cimatti & Daddi 2000; Stiavelli & Treu 2001; Cimatti et al. 2002a; Mannucci et al. 2002).

ERGs represent a key case in the knowledge of the cosmic history of star formation. In fact, old, massive ellipticals at $z > 1$ represent a problem for the standard hierarchical merging scenario of galaxy formation and evolution (White & Frenk 1991), where the most massive galaxies are assembled through a merging tree of less massive systems, even though the bulk of their stars may already be very old at the time of the last major merging (e.g. Kauffmann, Charlot & White 1996; Springel & Hernquist 2003). Conversely, the association of ERGs with DSGs at intermediate redshifts does not necessarily favour the latter scenario, if galaxies are assembled within times comparable to their star formation time-scales and the latter are shorter the larger the masses of the galaxies are, as independently proposed for late- (Gavazzi, Pierini & Boselli 1996) and early-type galaxies (Thomas, Maraston & Bender 2002). Interestingly 'hyper' ERGs have been interpreted as primodial ellipticals in a dusty starburst phase at $z \sim 3$ (Totani et al. 2001).

Unfortunately the classification either as a passively evolving, old elliptical or as a dusty starburst galaxy at $z > 1$ is uncomfortably ambiguous in the absence of an extensively observed SED (e.g. Smith et al. 2001), but the required observations are extremely challenging at present, given the faintness of the ERGs (e.g. Cimatti et al. 1999). Hence Pozzetti & Mannucci (2000, hereafter referred to as PM00) have proposed a classification criterion based on the relatively easily obtainable optical/near-IR photometry, particularly suitable for large samples of EROs with $K < 20$–21. This classification criterion is based on the rather neat difference in the distribution of the PM00 model ellipticals and DSGs at $1 < z < 2$ in the $I_c - K$ (or $R_c - K$) versus $J - K$ colour–colour diagram. This separation is mainly due to the fact that passively evolving, old stellar populations at these redshifts have their strong 4000-Å break redshifted to $\lambda < 1.2$ μm (J band), while coeval dusty galaxies show smoother SEDs and therefore redder observed $J - K$ colours, whatever the dust/stars configuration.

For the dusty ERGs, there is no unanimous consensus on the typical dustiness and star formation rate. The detection of ERO J164502+4626.4 ($z = 1.44$) at 850 μm (Cimatti et al. 1998) suggested that dusty ERGs may host massive quantities of dust accompanied by very high SFRs, as in ultraluminous infrared galaxies (ULIRGs) (see also Cimatti et al. 1997; Elbaz et al. 2002). Independently, 1.4-GHz radio maps reveal that $\geqslant 16 \pm 5$ per cent of the ERGs with $K < 20.5$ have radio luminosities expected for ULIRGs at $z \sim 1$ (Smail et al. 2002). Conversely, Andreani et al. (1999) and Mohan et al. (2002) conclude that approximately 20 per cent of the bright ($K < 19.5$–20) ERGs show strong submillimetre emission but that the dominant population of dusty, bright ERGs is probably made of starburst galaxies with a total mid-IR–millimetre rest-frame luminosity lower than 10^{12} $L_\odot$ and SFR $<$ few $\times$ 10^2 $M_\odot$ yr^{-1} (i.e. non-ULIRGs).

Here we re-address the optical/near-IR photometric classification of ERGs and investigate the relation between reddening, dustiness and SFR in dusty ERGs. This study has four main new points. First, we consider the presence of *stellar populations that are formed in a burst of short (0.1-Gyr) duration and are observed at* $1 < z < 2$ *in an early post-starburst phase while still embedded in a dusty medium*. Secondly, we consider the presence of passively evolving, old, *dusty elliptical galaxies* at $1 < z < 2$ as additional candidate ERGs. Thirdly, the treatment of dust attenuation follows the Monte Carlo simulations of the radiative transfer by Witt & Gordon (2000, hereafter referred to as WG00) for starbursts and post-starbursts, and those of Witt, Thronson & Capuano (1992, hereafter referred to as WTC92) for ellipticals. *For DSGs and dusty post-starburst galaxies (DPSGs), these models explore the dependence of dust attenuation on wavelength as a function of a dust/stars configuration, structure of the dusty medium and dust properties, which were not considered simultaneously or at all by PM00* (see Section 2.2.2). Fourthly, we calculate the total emission from dust in the mid-IR–(sub)millimetre wavelength range for DSGs/DPSGs.

2 MODELLING PASSIVELY EVOLVING, OLD ELLIPTICAL GALAXIES AND DUSTY STARBURST/POST-STARBURST GALAXIES AT $1 < Z < 2$

For our candidate ERGs (passively evolving, old ellipticals and DSGs/DPSGs), we consider three representative redshifts ($z = 1.07$, 1.39 and 1.85), consistent with published results. We adopt the so-called 'concordance' cosmological model ($\Omega_m = 0.3$, $\Omega_\lambda = 0.7$) with Hubble constant $H_0 = 70$ km s^{-1} Mpc^{-1} to link the redshift and the age of the models.

We use two evolutionary synthesis codes (one for ellipticals and one for DSGs/DPSGs) and fix metallicity (i.e. solar – $Z_\odot$) and the initial mass function (Salpeter 1955), since PM00 made an exhaustive investigation of the influence of these parameters on the colours of their candidate ERGs. However, we will discuss the impact of subsolar metallicities on our results.

Our focus is on the $I_c - K$, $R_c - K$ and $J - K$ colours, where Cousins (1976) I_c and R_c filters and Bessel & Brett (1988) J and K filters are used.

2.1 Passively evolving, old elliptical galaxies

2.1.1 Stellar populations

As in PM00, passively evolving, old ($\geqslant$1 Gyr) elliptical galaxies are simulated through simple stellar population (SSP) models. Hereafter they are referred to as Es for simplicity. Their intrinsic (i.e. unattenuated by dust) SEDs are computed with the evolutionary synthesis code of Maraston (1998).

We assume a maximal formation redshift $z_f = 10$, against the three values of formation redshift (i.e. $z_f = 3$, 4 and 6) assumed by PM00 for their model Es. An elliptical galaxy formed at $z_f = 10$ has an age of approximately 5, 4 and 3 Gyr at $z = 1.07$, 1.39 and 1.85, respectively. One formed at $z_f = 3$ (PM00; see also Totani et al. 2001) has an age of approximately 3.4, 2.4 and 1.4 Gyr at $z = 1.07$, 1.39 and 1.85, respectively.

We note that a 1-Gyr old galaxy at $z = 1.07$, 1.39 or 1.85 was formed at $z_f = 1.39$, 1.85 or 2.59, respectively. Thus a 1-Gyr old elliptical at $1 < z \leqslant 1.5$ may have its progenitor in the redshift range that we are interested in. Hence it is important to investigate the case of a post-starburst galaxy and illustrate the difference

between a model DPSG and a model elliptical galaxy of similar young/intermediate age (see Section 2.2.1).

For model Es we adopt a minimum stellar mass of 7.5×10^{10} $M_\odot$, which is approximately the residual (i.e. after 25 per cent mass loss owing to stellar evolution) stellar mass of a 1-Gyr old SSP (from Maraston 1998) and of a 1-Gyr old model DSG/DPSG (cf. Section 2.2.1), both originating from a 10^{11}-$M_\odot$ cloud of primordial gas.

2.1.2 Dust attenuation

We test the impact of dust attenuation on the observed SEDs of Es at $1 < z < 2$. The residual interstellar medium of a dusty elliptical is considered to be negligible with respect to its characteristic stellar mass.

For dusty Es we adopt the dust attenuation curves obtained from the Monte Carlo simulations of the radiative transfer by WTC92 for the CLOUDY geometry (see also WG00). This geometry assumes a spherical stellar distribution that declines from the core as r^{-3} and a *homogeneous Milky Way-type dust present only in the inner portions of the model*, extending from the centre to two-thirds of the galaxy radius and following a distribution that declines as r^{-1}. The results of this model are robust when different radial dependences of the stellar and dust distributions are assumed (cf. Bianchi, Ferrara & Giovanardi 1996; Wise & Silva 1996; WG00).

The value of the radial extinction optical depth from the centre to the edge of the dust environment at V band, assuming a constant density, homogeneous distribution, (τ_V) is set to 0.5, consistent with the mean τ_V estimated from the analysis of broad-band colour gradients in nearby Es (WTC92; Wise & Silva 1996). These studies provide upper limits to τ_V, since they do not take into account intrinsic gradients in metallicity of the stellar populations of Es (e.g. Saglia et al. 2000).

In Fig. 2 (see Section 2.2.2), we reproduce the attenuation function,[1] normalized to its V-band value ($A_\lambda{}^{\rm norm}$) of dusty Es for $\tau_V = 0.5$, which produces a value of the stellar reddening $[E(B-V)_{\rm star}]$ equal to 0.15.

2.2 Dusty starburst/post-starburst galaxies

2.2.1 Stellar populations

Intrinsic SEDs of young ($\leqslant$0.1 Gyr)/intermediate-age (0.1–1 Gyr) starburst and intermediate-age post-starburst galaxies are computed with the evolutionary synthesis code (version 2.0) PÉGASE (Fioc & Rocca-Volmerange 1997), because this code includes nebular emission. PÉGASE 2.0 does not include the TP-AGB phase that is dominant at intermediate ages, but this fact does not represent a major problem since we are considering observed wavelengths shorter than 2.2 μm (K band).

Gas is assumed to be transformed into $Z_\odot$ stars at a constant rate over a period $t_{\rm burst}$ of 0.1 Gyr (short burst) or 1 Gyr (long burst) at $1 < z < 2$. For a total mass of transformed gas $M_{\rm gas} = 10^{11}$ $M_\odot$, an SFR equal to $M_{\rm gas}/t_{\rm burst}$ corresponds to 10^2 $M_\odot$ yr^{-1} (long burst) or 10^3 $M_\odot$ yr^{-1} (short burst). Note that SFRs $\sim 10^3$ $M_\odot$ yr^{-1} have been inferred from observations of high-z SCUBA submillimetre sources (e.g. Smail, Ivison & Blain 1997; Barger et al. 1998; Cimatti et al. 1998; Hughes et al. 1998; Eales et al. 1999; Bertoldi et al. 2000; Lutz et al. 2001; Smail et al. 2003).

These star formation histories and SFRs are complementary to those adopted by PM00 for their DSGs for the following reason. *The constant star formation rate from a formation redshift 2.5 or, especially, 6, assumed by PM00 for their basic model of a DSG, better corresponds to a continuously star-forming galaxy with an intermediate/low SFR at* $1 < z < 2$. An object formed at $z_{\rm f} = 2.5$ (6) is approximately 0.7 (2.3) Gyr old at $z = 2$, and 3.2 (4.8) Gyr old at $z = 1$, for the same cosmology as in Section 2. Hence it may hardly sustain a constant SFR larger than 10^2 $M_\odot$ yr^{-1} for such long times. For our DSGs/DPSGs observed at $z = 1.07$, 1.39 or 1.85, the maximum age of 1 Gyr corresponds to a maximum $z_{\rm f}$ of 1.39, 1.85 or 2.59, respectively. Hence *these systems are mostly formed at* $1 < z < 2$. We consider additional model ages of 50, 100, 200, 300 and 500 Myr.

PM00 also consider model starbursts with an SFR having an e-folding time of 100 Myr. These PM00 models are consistent with our models of starbursts with a short burst at an age of 100 Myr. However, PM00 do not consider an early post-starburst phase at $1 < z < 2$.

At this point the difference between a post-starburst galaxy and a passively evolving elliptical galaxy younger than 1 Gyr may sound a matter of semantics, since a DSG at $1 < z < 2$ may evolve into an elliptical at $z = 0$ and, eventually, already at these redshifts. As far as stellar properties are concerned, the SED of post-starburst stellar population under investigation and of an SSP with the same age and metallicity, identified as a passively evolving elliptical galaxy, are different (as expected) even after 1 Gyr from the onset of star formation, as shown in Fig. 1. However, it is the presence,

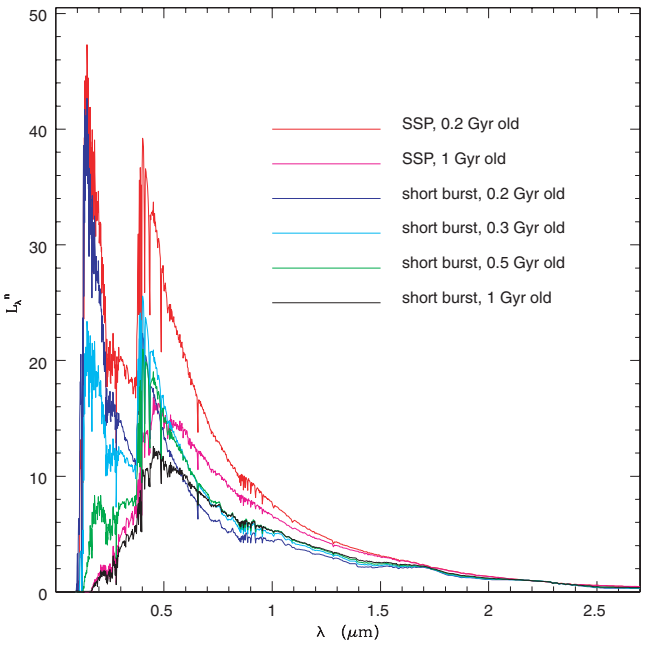

Figure 1. The intrinsic SED of an SSP with $Z_\odot$ and age equal to 0.2 (red line) or 1 Gyr (magenta line) and the intrinsic SED of a stellar population originated in a 100-Myr burst with $Z_\odot$ and age equal to 0.2 (blue line), 0.3 (cyan line), 0.5 (green line) or 1 Gyr (black line). Each SED is in the rest frame of the object and is normalized to the luminosity at 2.17 μm. It is evident that these two sets of SEDs are different at any intermediate age.

[1] We stress the difference between the dust extinction curve and the dust attenuation curve. The former describes the absorption and scattering properties of a mix of dust grains of given size distribution and chemical composition as a function of wavelength; the latter is the convolution of the extinction curve with the geometry of the dusty stellar system. The attenuation curve depends on the structure of the dusty medium and the amount of dust.

distribution and structure of the (dusty) interstellar medium which provides fundamental physical differences between these two stellar systems in our models.

The mass fractions of stars and residual gas are 74 (77) per cent and 22 (19) per cent, respectively, for a 1-Gyr old stellar system formed in a short (long) burst. For DSGs with a short burst, these fractions are 87 and 11 per cent, respectively, at the end of the burst (i.e. at an age of 100 Myr). We assume that gas and dust components survive at least partly in model DSGs/DPSGs for the largest time window (1 Gyr) considered for these objects (see Section 2.2.3). The fate of these components afterwards may channel the evolution of these starbursts towards either a 'gas-poor' system (i.e. an early-type galaxy) or a 'gas-rich' one (i.e. a late-type galaxy) at $z = 0$, both systems having a stellar mass of $\sim 10^{10}$–10^{11} $M_\odot$.

Thus a 1-Gyr old DPSG at $z = 1.85$ could be the transition evolutionary phase of elliptical dusty formation occurred at intermediate redshift ($z = 2$–3) (Granato et al. 2001; Totani et al. 2001). However, the dusty formation of more massive Es at intermediate redshift would require initial starbursts with SFR $\geqslant 10^3$ $M_\odot$ yr^{-1} and/or $t_{\rm burst} \geqslant 100$ Myr (cf. Granato et al. 2001).

2.2.2 *Dust attenuation*

Gordon, Calzetti & Witt (1997, hereafter referred to as GCW97) have investigated the nature of the dust in starbursts by constructing different models of the stars and dust in DSGs, combining stellar evolutionary synthesis and radiative transfer through dust, and applying them to the observed ultraviolet (UV)/optical colours of 30 nearby starburst galaxies of the Calzetti sample (Calzetti, Kinney & Storchi-Bergmann 1994). Their main conclusion are as follows.

(i) Starburst dust has an extinction curve lacking the 2175-Å bump, such as the Small Magellanic Cloud (SMC) curve and at variance with the Milky Way (MW) curve, and a steep far-UV rise, intermediate between these two curves. This is consistent with the conclusion of Calzetti et al.

(ii) The dust/stars geometry that better explains the distribution of these 30 starbursts in various UV/optical colour–colour plots has an inner dust-free sphere of stars surrounded by an outer star-free shell with a two-phase clumpy, dusty medium. A geometry where dust and stars are uniformly mixed throughout the entire sphere cannot explain the spread in the UV/optical colours, whether its local distribution of dust is homogeneous or clumpy.

Models of dusty starbursts based on similar considerations reproduce the optical colour–redshift distribution of Lyman-break galaxies well at $2 < z < 4$ (Vijh, Gordon & Witt 2003). In addition, Cimatti et al. (1997) suggest that the stellar component of ERO J164502+4626.4 should be strongly embedded in the dust in order to reproduce its observed extremely red colour.

For all of these reasons, we apply the Monte Carlo simulations of the radiative transfer by WG00 for the SHELL geometry to DSGs/DPSGs at $1 < z < 2$. This geometry assumes *a dust/stars distribution where the stars extend to 0.3 of the system radius and the dust extends from 0.3 to 1 of the system radius*. The dust in the shell is distributed in a *two-phase clumpy medium*, composed of molecular clouds and diffuse gas, where the filling factor of the clumps is set to 0.15 and the low-density to high-density ratio is set to 0.01. We consider the additional extreme hypothesis that dust is locally distributed in a single, *homogeneous medium*.

We assume an *SMC-like extinction curve* and consider values of τ_V equal to 0.25, 0.5, 1, 2, 3, 4, 5, 6, 8, 10, 20, 30, 40 and 50 for the two-phase clumpy dust distribution and equal to 0.25–8 for the homogeneous one. Here we recall that τ_V *gives the total amount of dust* in the shell, since the dust column density is proportional to $\tau_V a\rho$, where a is the characteristic grain size and ρ is the density of the grain material. Values of τ_V at the low and high end of the distribution seem to be characteristic of starbursts and ULIRGs, respectively, at low and high z (e.g. Vijh et al. 2003 and references therein).

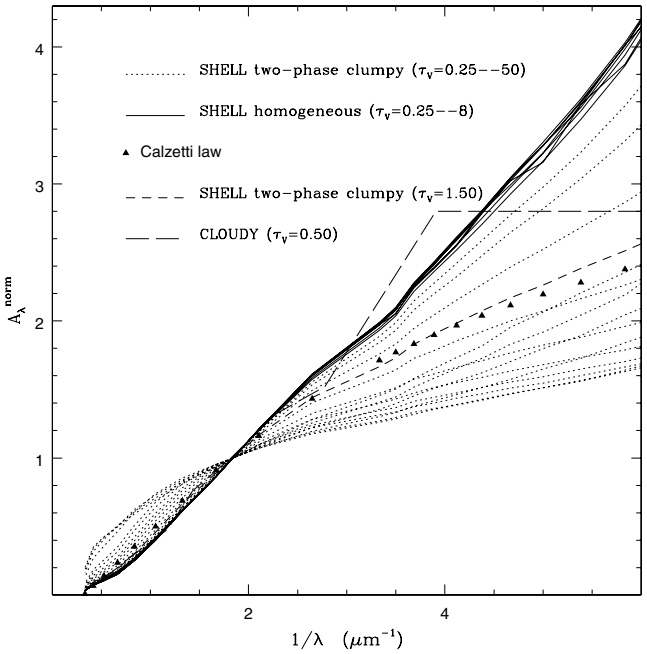

Figure 2. The attenuation function, normalized to its V-band value (i.e. $A_\lambda{}^{\rm norm}$) for: (a) the WTC92 cloudy geometry of a dusty elliptical galaxy with MW-type dust and $\tau_V = 0.5$ (long-dashed line); (b) the WG00 SHELL geometry of a DSG with SMC-type dust (solid or dotted lines for a homogeneous or two-phase clumpy dust distribution, respectively) and different values of τ_V. As a reference, we reproduce the normalized attenuation function for the WG00 SHELL model with clumpy SMC-type dust and $\tau_V = 1.5$ (short-dashed line), which is consistent with the normalized Calzetti law (filled triangles).

We also assume that the gas emission at a given wavelength is attenuated by the same amount as the stellar emission at that wavelength, whether the gas emission is either in a line or in the continuum. This is at odds with the result that the stellar continuum suffers roughly half of the reddening suffered by the ionized gas (Fanelli, O'Connell & Thuan 1988; Mas-Hesse, Arnault & Kunth 1989; Calzetti et al. 1994) but the understanding of the attenuation of the ionized-gas line emission from dust is still controversial. However, *the following results hold when no nebular emission is taken into account*, as demonstrated in Appendix A.

Fig. 2 reproduces the attenuation curves (normalized to V band) for the SHELL dust/stars configuration and SMC-type dust locally distributed in a homogeneous (solid lines) or two-phase clumpy medium (dotted lines) as a function of τ_V. It also shows the values of the normalized attenuation function of nearby starbursts (Calzetti et al. 2000), known as the 'Calzetti law', for the WG00 wavelengths (filled triangles).

Two important results are contained in Fig. 2. First, the attenuation function for the SHELL geometry with a two-phase clumpy distribution of SMC-type dust and $\tau_V = 1.5$ reproduces rather well the calibrated Calzetti law for nearby starbursts, as already shown

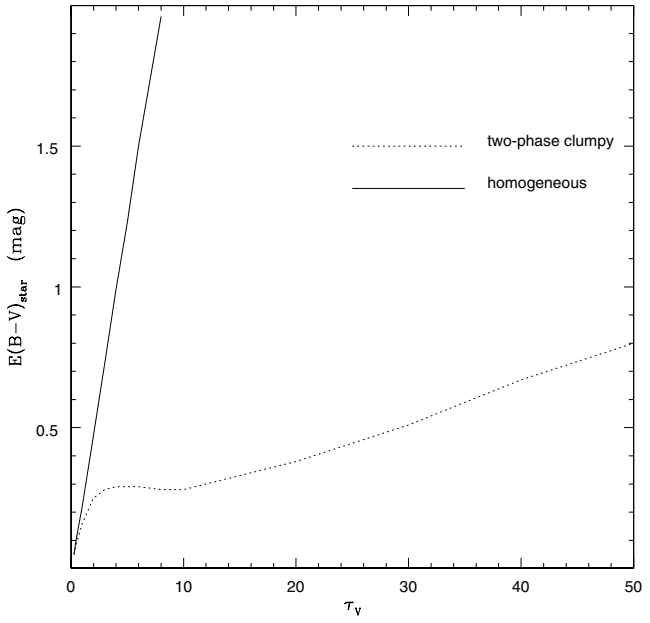

Figure 3. Stellar reddening $E(B-V)_{\rm star}$ versus τ_V for the SHELL geometry of a DSG with SMC-type dust distributed in a homogeneous (solid line) or two-phase clumpy (dotted line) medium.

by Vijh et al. (2003). Nevertheless, a wide range of different attenuation curves may apply to individual DSGs/DPSGs, as a function of local distribution of the dust and dust content. We discuss the effect of using the empirically determined Calzetti law for whatever dusty ERG (e.g. Cimatti et al. 2002a) in Appendix B.

Secondly, *the shape of the attenuation function depends on the structure of the dusty medium and, in the two-phase clumpy case, on* τ_V. Changes in normalization also exist, in both cases, of course (not shown). In particular, a homogeneous dusty medium provides a larger attenuation at any wavelength than a two-phase clumpy one with the same τ_V.

In addition, we stress that *the relation between* $E(B-V)_{\rm star}$ *and the amount of dust (i.e.* τ_V*) is usually quite non-linear and highly dependent on details of the structure of the dusty medium*, as shown in Fig. 3. The existence of an initial 'plateau' in $E(B-V)_{\rm star}$ versus τ_V in the two-phase clumpy case is due to fact that individual clumps become optically thick while the low-density interclump medium initially contributes little to the reddening.

Finally, we note that, apart from the observationally established attenuation function of Calzetti (1997) (see Appendix B), all the model attenuation functions considered by PM00 do not contemplate dust with an SMC-type extinction curve and distributed in a two-phase clumpy medium *at the same time*, and a SHELL-like geometry. We anticipate that these important differences do not affect our re-analysis of the two-colour classification criterion for ERGs. In fact, our results are consistent with those of PM00 when continuously star-forming DSGs are considered, whatever structure of the dusty medium is assumed.

2.2.3 The physics behind the SHELL configuration

The existence of dust in young galaxies is expected because Type II supernovae (SNe II) are shown to produce dust grains (e.g. Dwek et al. 1983; Moseley et al. 1989; Kozasa, Hasegawa & Nomoto 1991; Todini & Ferrara 2001). Dust production from SNe II follows the formation and evolution of massive stars on a nuclear time-scale (few $\times 10^6$ yr). Mass loss from evolved intermediate-mass stars contributes to dust formation as well (Gehrz 1989) and follows the slower evolutionary time-scales of these stars (from $\sim 10^8$ to $\sim 10^9$ yr). Dust is also destroyed by SN shocks (McKee 1989; Jones, Tielens & Hollenbach 1996). Nevertheless, the detailed modelling of dust evolution in high-z and nearby young starbursts shows that it is possible to build up a dust mass within a factor of 2 of the total within a few $\times 10^7$ yr (Hirashita & Ferrara 2002; Hirashita, Hunt & Ferrara 2002). Early dust is similar to that of the SMC (Takeuchi et al. 2003).

Dust and residual gas face displacement and, eventually, partial/total removal from the system owing to the onset of galactic winds powered by SN explosions and acceleration up to velocities of several $\times 10^3$ km s^{-1} (e.g. Suchkov et al. 1994, 1996; Shu, Mo & Mao 2003). In the case of dust grains, destruction by sputtering must be taken into account (e.g. Ellison, Drury & Meyer 1997). SN Ia will contribute to dust destruction/displacement in addition to SN II, because their time-scales span a wide range: roughly 60 per cent of Type Ia SN progenitors have lifetimes $\sim$3–4 $\times$ 10^8 yr, while 30 per cent of them are expected to be very old (10^9–10^{10} yr) (Branch et al. 1995). The existence of galactic superwinds associated with dust extends from nearby to high-z starbursts (Heckman 2001 and references therein; Adelberger et al. 2003).

The fate of the surviving ejected dust grains is uncertain for the following reasons. The ambient halo gas that the superwind shocks and the dense disc gas that it entrains travel at velocities of a few $\times 10^2$ km s^{-1}, which are near to typical escape velocities (Nakai et al. 1987; Phillips 1993). Furthermore, displaced grains may respond as much to radiation pressure (Norman & Ferrara 1996; Davies et al. 1998) as they do to gas pressure (and to any poloidal magnetic field that might be present – Beck et al. 1994). Hence displaced dust may decouple from the gas so that its path through the halo becomes even more uncertain. Displaced grains may partially undergo both reconnection to the original disc and removal from the system, and they may exist in equilibrium positions above the plane of the galaxy (Davies et al. 1998; see also Greenberg et al. 1987; Barsella et al. 1989). This supports our assumption that the SHELL geometry also applies to the immediate post-burst phase of a DSG.

3 PREREQUISITES FOR A MODEL BEING AN ERO

Existing ground-based near-IR surveys (Drory et al. 2001; Cimatti et al. 2002b; Smail et al. 2002) reach a typical limit of $K = 20.5$. $K < 20$–21 is also the limit of validity of the PM00 method, introduced by these authors in order to avoid statistical contamination by $z > 2$ ellipticals in the optical/near-IR colour–colour region populated by DSGs.

An important prerequisite of our models is to match observed photometric properties of EROs, i.e. $K < 20.5$ and, for example, $4 \leqslant I_c - K < 8$. Thus we show the distribution in the $I_c - K$ versus K colour–magnitude plane of our models of Es, DSGs with a short burst and DPSGs, and DSGs with a long burst in Figs 4–6, respectively.

Here we remind the reader that our model Es have a minimum stellar mass equal to 7.5×10^{10} M$_\odot$ whatever the age (from 1 to 3–5 Gyr). Model DSGs with a short burst have stellar masses equal to 4.5 and 8.7×10^{10} M$_\odot$ when they are 0.05 and 0.1 Gyr old, respectively, while model DPSGs have stellar masses equal to 8.1, 7.9, 7.7 and 7.4×10^{10} M$_\odot$ when they are 0.2, 0.3, 0.5 and 1 Gyr old, respectively. Finally, DSGs with a long burst have stellar masses

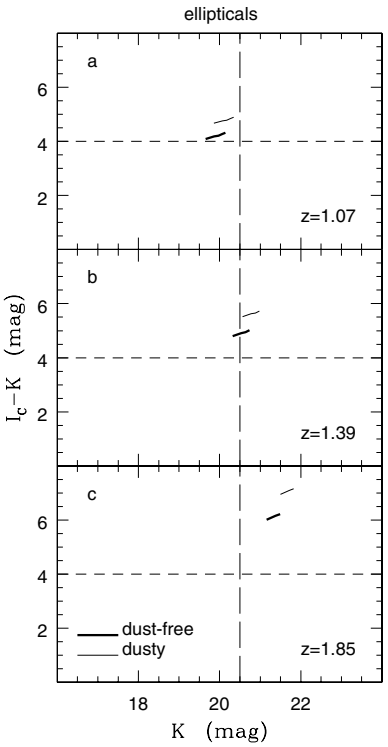

Figure 4. Distribution of model Es at $z = 1.07$ (a), $z = 1.39$ (b) or $z = 1.85$ (c) in the $I_c - K$ versus K colour–magnitude diagram for the dust-free (thick solid line) or dusty (thin solid line) case. In each panel, the model age increases from left to right along each line. Long- and short-dashed lines reproduce the limiting magnitude of current ERO samples and the $I_c - K$ colour selection criterion for EROs, respectively. Note the extremely narrow locus populated by Es at $1 < z < 2$ in this plane.

equal to 0.4, 0.9, 1.7, 2.5, 4.0 and 7.7×10^{10} $M_\odot$ when they are 0.05, 0.1, 0.2, 0.3, 0.5 and 1 Gyr old, respectively.

From Fig. 4 it is evident that model dust-free Es of 7.5×10^{10} $M_\odot$ correspond to observed EROs only if they are at $z < 1.4$ (for any age at $z \sim 1$ or for ages less than 2 Gyr at $z \sim 1.4$). Dusty Es of the same stellar mass correspond to observed EROs only if they are at $z \sim 1$ (for any age). Hence stellar mass plays a key role: a 10 times more massive passively evolving, old elliptical galaxy at $1 < z < 2$ is always a candidate ERO, whether dusty or not. Indeed, large near-IR surveys aimed at testing galaxy formation models are designed to detect Es more massive than $\sim 10^{11}$ $M_\odot$ at high z (e.g. Drory et al. 2001).

The prerequisites for a model DSG/DPSG at $1 < z < 2$ being a candidate observed ERO are more complex, as illustrated in Figs 5 and 6 and summarized in Table 1. This is largely due to the well-known existence of the age/opacity degeneracy (Takagi, Arimoto & Vansevicius 1999 and references therein).

A dusty stellar system originating in a 100-Myr burst evolves towards redder $I_c - K$ colours when it ages, for fixed dust distribution and amount of dust. It also evolves towards brighter K magnitudes for the first 100 Myr and towards fainter K magnitudes during the following post-starburst phase. Conversely, it becomes fainter in K and redder in $I_c - K$ when τ_V increases, for a fixed age. In general, younger starbursts with $t_{\rm burst} = 100$ Myr must be more attenuated in order to match the properties of observed EROs, be their dusty medium two-phase clumpy or homogeneous (Fig. 5). In the second case, a lower amount of dust is needed in order to produce a given reddening (cf. Fig. 3).

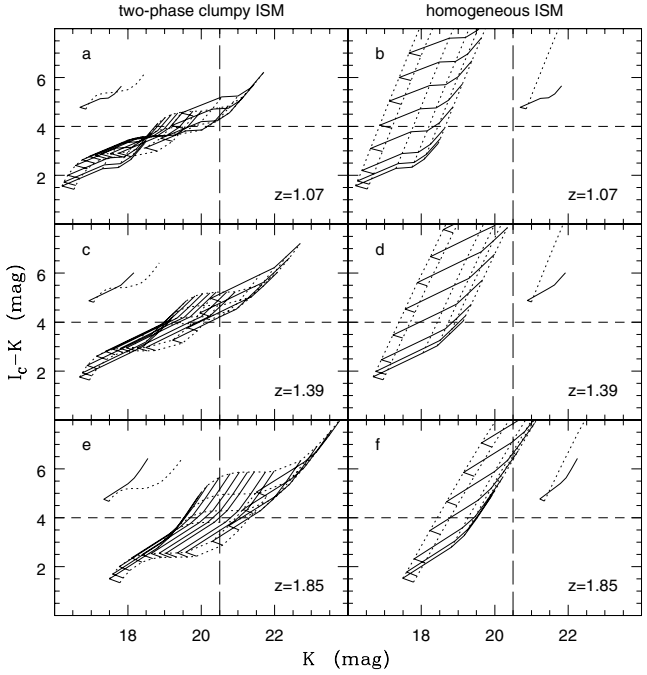

Figure 5. Distribution of model DSGs with a short burst and DPSGs at $z = 1.07$ (a, b), $z = 1.39$ (c, d) or $z = 1.85$ (e, f) in the $I_c - K$ versus K colour–magnitude plane for the two-phase clumpy (a, c, e) and homogeneous (b, d, f) dust distributions. Long- and short-dashed lines are the same as in Fig. 4. Solid or dotted lines connect models with constant τ_V or age, respectively. In the upper left-hand (right-hand) corners of a, c, e (b, d, f) we reproduce the typical trend of models with increasing age (solid line) or increasing τ_V (dotted line) – see the text.

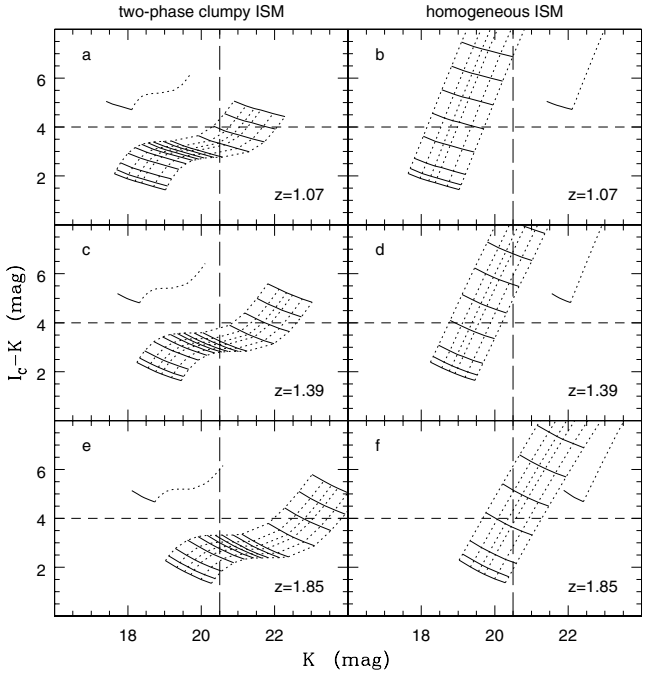

Figure 6. The same as in Fig. 5 but for model DSGs with a long burst. Solid or dotted lines connect models with constant τ_V or age, respectively. In the upper left-hand (right-hand) corners of a, c, e (b, d, f) we reproduce the typical trend of models with increasing age (solid line) or increasing τ_V (dotted line) – see the text.

Table 1. Parameters of model DSGs/DPSGs selected as EROs with $K < 20.5$.

$t_{\rm burst}$ Myr	Age Myr	Two-phase clumpy	Homogeneous	z
100	50	$\tau_V > 40$	$3 < \tau_V < 8$	1.07
100	100	$\tau_V \geqslant 40$	$3 \leqslant \tau_V < 8$	1.07
100	200	$20 < \tau_V < 50$	$2 < \tau_V < 8$	1.07
100	300	$20 < \tau_V < 40$	$2 < \tau_V < 8$	1.07
100	500	$10 < \tau_V < 30$	$2 \leqslant \tau_V \leqslant 6$	1.07
100	1000	$1 < \tau_V < 20$	$1 < \tau_V < 6$	1.07
100	50	$\tau_V > 30$	$2 < \tau_V \leqslant 6$	1.39
100	100	$30 < \tau_V \leqslant 50$	$2 < \tau_V \leqslant 6$	1.39
100	200		$1 < \tau_V < 6$	1.39
100	300	$2 < \tau_V < 20$	$1 < \tau_V \leqslant 5$	1.39
100	500	$1 < \tau_V \leqslant 10$	$1 \leqslant \tau_V < 5$	1.39
100	1000	$0.25 \leqslant \tau_V < 8$	$0.25 \leqslant \tau_V \leqslant 4$	1.39
100	50		$2 < \tau_V < 6$	1.85
100	100		$2 < \tau_V < 6$	1.85
100	200		$1 < \tau_V \leqslant 4$	1.85
100	300	$1 < \tau_V \leqslant 5$	$1 \leqslant \tau_V < 4$	1.85
100	500	$0.25 < \tau_V \leqslant 3$	$0.25 \leqslant \tau_V < 3$	1.85
100	1000	$\tau_V \leqslant 2$	$\tau_V < 2$	1.85
1000	50		$3 \leqslant \tau_V \leqslant 6$	1.07
1000	100		$3 \leqslant \tau_V < 8$	1.07
1000	200		$2 < \tau_V < 8$	1.07
1000	300		$2 < \tau_V < 8$	1.07
1000	500		$2 < \tau_V < 8$	1.07
1000	1000	$\tau_V \sim 30$	$2 < \tau_V < 8$	1.07
1000	50		$2 < \tau_V < 4$	1.39
1000	100		$2 < \tau_V < 5$	1.39
1000	200		$2 < \tau_V \leqslant 5$	1.39
1000	300		$2 < \tau_V < 6$	1.39
1000	500		$2 < \tau_V < 6$	1.39
1000	1000		$2 \leqslant \tau_V < 6$	1.39
1000	300		$2 < \tau_V < 3$	1.85
1000	500		$2 \leqslant \tau_V \leqslant 3$	1.85
1000	1000		$1 < \tau_V < 4$	1.85

A DSG with a 1-Gyr burst evolves towards brighter K magnitudes and redder $I_c - K$ colours when it ages, for fixed dust distribution and amount of dust. Conversely, it becomes fainter in K and redder in $I_c - K$ when τ_V increases, for a fixed age. Interestingly, starbursts with $t_{\rm burst} = 1$ Gyr do not match observed ERGs if their dusty medium is two-phase clumpy (in the way we assumed in Section 2.2.2) if not at $z \sim 1$ and for an age of 1 Gyr and $\tau_V \sim 30$ (Fig. 6). They also hardly satisfy the ERO selection criterion at any age, if not for large amounts of dust (i.e. for $\tau_V > 20$). Conversely, DSGs with long bursts and a homogeneous dusty medium fall in the region populated by observed ERGs for low/intermediate amounts of dust and almost any age, at any redshift between 1 and 2. For these models the range in dustiness or age allowed by observations increases with decreasing z. We conclude that the model DSGs/DPSGs at $1 < z < 2$ span very well the region of the $I_c - K$ versus K colour–magnitude plane populated by observed ERGs.

At this point it is interesting to note what happens if a 10 times lower mass (i.e. equal to 10^{10} $M_\odot$) of primordial gas is transformed into stars at a constant rate on a time-scale of 0.1 or 1 Gyr. In this case, we find that DSGs with a short (long) burst and SFR $= 10^2$ $M_\odot$ yr^{-1} (10 $M_\odot$ yr^{-1}) and their dusty post-starburst phases result to be too faint to be detected by present ground-based K-band surveys, whatever the redshift, the amount of dust and the distribution. Hence we conclude that these surveys are not sensitive to dusty formation of low-mass galaxies at $1 < z < 2$ (if any).

4 THE $I_C - K$ VERSUS $J - K$ COLOUR–COLOUR DIAGRAM

Hereafter we will discuss only the $I_c - K$ versus $J - K$ colour–colour diagram since similar conclusions hold for the $R_c - K$ versus $J - K$ colour–colour diagram.

The PM00 classification criterion for ERGs is

$$J - K = 0.36(I_c - K) + 0.46.$$

ERGs with given observed $I_c - K$ colour are classified as Es (DSGs) at $1 < z < 2$ if they have a bluer (redder) observed $J - K$ colour than this.

4.1 Dust effects on the colours of passively evolving, old, dusty ellipticals

Fig. 7 shows the distribution in the $I_c - K$ versus $J - K$ colour–colour plane of dust-free (filled symbols) and dusty (empty symbols) Es at $1 < z < 2$. The short-dashed and solid lines represent, respectively, the ERO selection function (i.e. $I_c - K \geqslant 4$) and the PM00 classification criterion for ERGs.

All the model Es obey the PM00 classification criterion for ERGs, i.e. they fall on the left-hand side of the delimiting line (solid line) in Fig. 7. This is reassuring for dust-free Es, since the evolutionary models examined by PM00 adopt the same stellar tracks, while those adopted here (Maraston 1998) rely on a different set of stellar models.

The new result is that models of dusty Es still fall on the left of the PM00 separation line, for reasonable upper limits to the amount of dust present in these stellar systems.

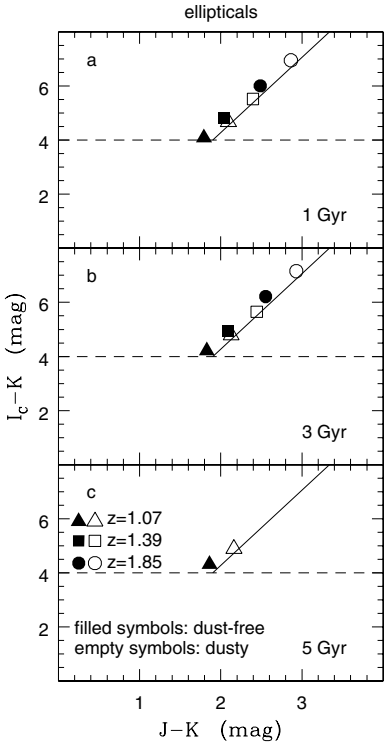

Figure 7. The distribution in the $I_c - K$ versus $J - K$ colour–colour plane of dust-free (filled symbols) and dusty (empty symbols) Es at $1 < z < 2$. In each panel model Es of selected ages are reproduced as triangles, squares and circles according to their redshifts. The short-dashed and solid lines represent, respectively, the ERO selection function and the PM00 classification criterion for ERGs. All model Es obey the latter criterion.

In general, the inclusion of dust attenuation moves the dust-free models in Fig. 7 towards redder $I_c - K$ and $J - K$ colours, almost parallel to the age-sequence track, for fixed metallicity, at a given redshift, and closer to the PM00 separation line, whatever the redshift and the age of the model elliptical galaxy. Thus dust attenuation in Es may explain very red $I_c - K$ and $J - K$ colours without the need of invoking extremely old ages or higher redshifts (or higher metallicities, cf. PM00).

4.2 Dusty starburst/post-starburst galaxies

Hereafter we refer to model DSGs with a 100-Myr burst and model DPSGs, both with a two-phase clumpy distribution of the dust, as *basic model DSGs* and *basic model DPSGs*, respectively, given the results of GCW97.

4.2.1 DSGs with a short burst and DPSGs

Fig. 8 reproduces the distribution of basic model DSGs/DPSGs with different age and the amount of dust in the $I_c - K$ versus $J - K$ colour–colour plane. It shows that DSGs with a 100-Myr burst at $1 < z < 2$ obey the PM00 classification criterion, whatever the structure of the dusty medium and the amount of dust.

Conversely, an intermediate age, dusty post-starburst galaxy may be mistaken for either a passively evolving, old elliptical or a young, dusty starburst, both at $1 < z < 2$, as a function of its redshift, when classified only on the basis of optical/near-IR colours such as $I_c - K$ (or $R_c - K$) and $J - K$.

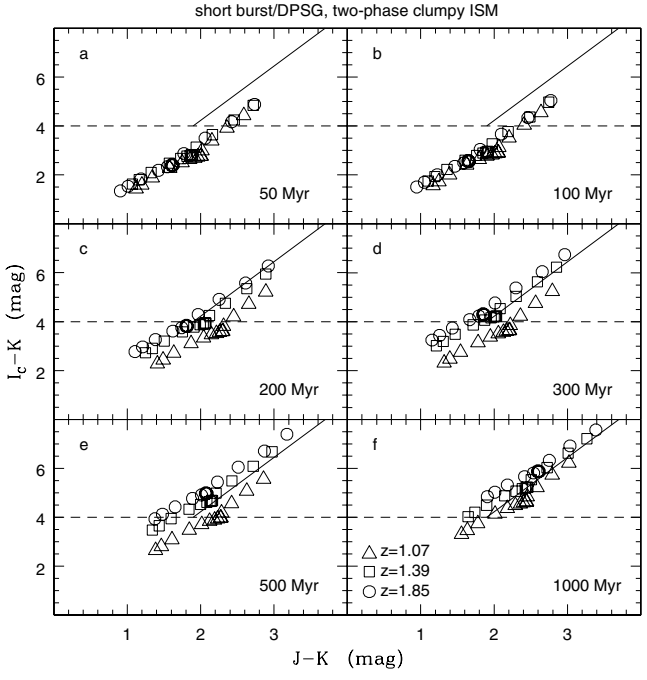

Figure 8. The distribution of the basic model DSGs/DPSGs in the $I_c - K$ versus $J - K$ colour–colour plane, where lines are the same as in Fig. 7. In each panel models of selected age are reproduced as triangles, squares or circles according to their redshifts, with τ_V increasing from 0.25 to 50 from the lower left to the upper right. Model DPSGs older than 200 Myr and with a large range in τ_V not only populate the region of DSGs (upper right-hand quadrant) but they also 'intrude' the region (upper left-hand quadrant) where only passively evolving, old, dust-free Es were expected to fall (PM00).

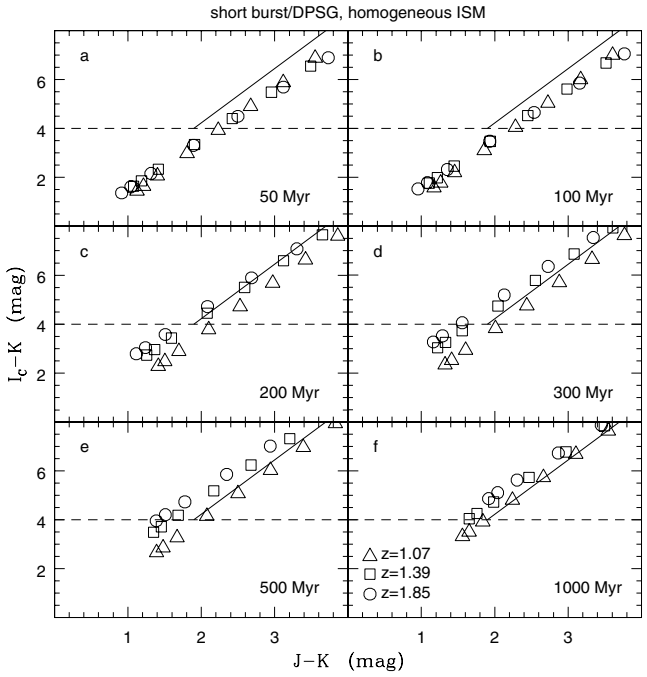

Figure 9. The distribution of DSGs with a short burst/DPSGs with a homogeneous dusty medium in the same plane as in Fig. 8. Each panel shows models of selected age at different z, with τ_V increasing from 0.25 to 8 from the lower left to the upper right. The 'intruder' (see the text) DPSGs with a homogeneous dusty medium have stellar populations similar to those of basic model DPSGs in Fig. 8.

In particular, basic model DPSGs with ages between 0.2 and 1 Gyr populate the region (upper left-hand quadrant in Fig. 8) where only dust-free Es were expected to fall, according to PM00 (see also Mannucci et al. 2002). These 'intruder' basic model DPSGs are at $1.3 < z < 2$ and span a large range in τ_V ($0.25 \leqslant \tau_V \leqslant 40$), according to age. These values of τ_V are not implausibly large, especially when the model DPSGs have a homogeneous dust distribution (Fig. 9). In this case, the reddening effect per given amount of dust is maximized (Fig. 3), so that these 'intruders' have $\tau_V \leqslant 5$ (according to redshift). We stress that the 'intruder' DPSGs may be luminous enough to be observed in present surveys at $K < 20.5$, whether the dust distribution is homogeneous or two-phase clumpy (cf. Table 1). Hence the presence of a dusty post-starburst phase at $1.3 < z < 2$ is a source of concern for the neat result of PM00.

Finally, we note that the mix of DPSGs with ages between 0.2 and 1 Gyr at $z \sim 1$ and DSGs (with ages between 0.05 and 0.1 Gyr) at $1 < z < 2$ in Fig. 8 is due to a conspiracy between redshift, shape of the intrinsic SED and behaviour of the attenuation function of these stellar systems. The class of DPSGs is a suitable candidate for interpreting the low dust emissions attributed to the bulk of dusty, bright EROs on the basis of submillimetre observations (cf. the introduction), as detailed in Section 5.

4.2.2 DSGs with a long burst

Figs 10 and 11 show that model DSGs forming stars continuously in a long burst satisfy the PM00 classification criterion, whether or not the dust distribution is two-phase clumpy (but these models are too faint in K to be selected as EROs – see Fig. 6) or homogeneous, respectively. PM00 have considered analogous starbursts observed during continuous star formation activity.

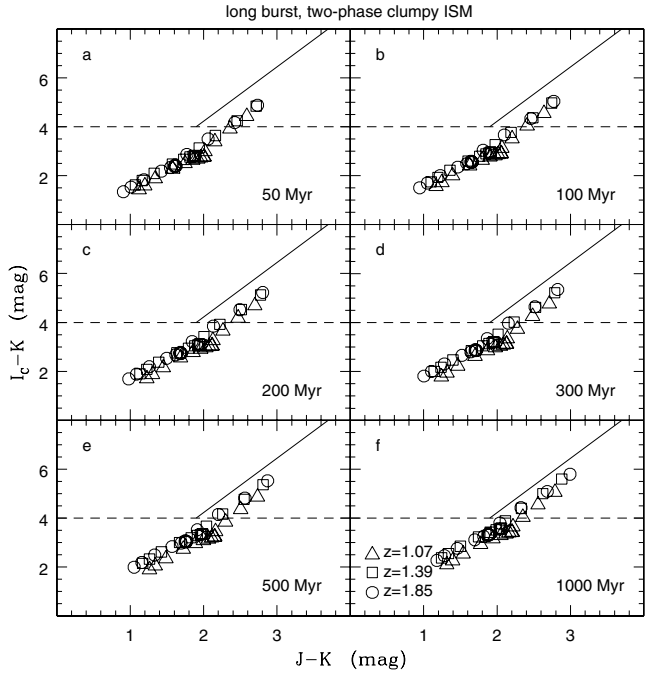

Figure 10. The distribution of model DSGs with a 1-Gyr burst and a two-phase clumpy dust distribution in the $I_c - K$ versus $J - K$ colour–colour plane as a function of age and z. In each panel τ_V increases from 0.25 to 50 from the lower left to the upper right. Lines and symbols are the same as in Fig. 8. These DSGs meet the PM00 classification criterion for ERGs, even though they are too faint to be selected as EROs (Fig. 6).

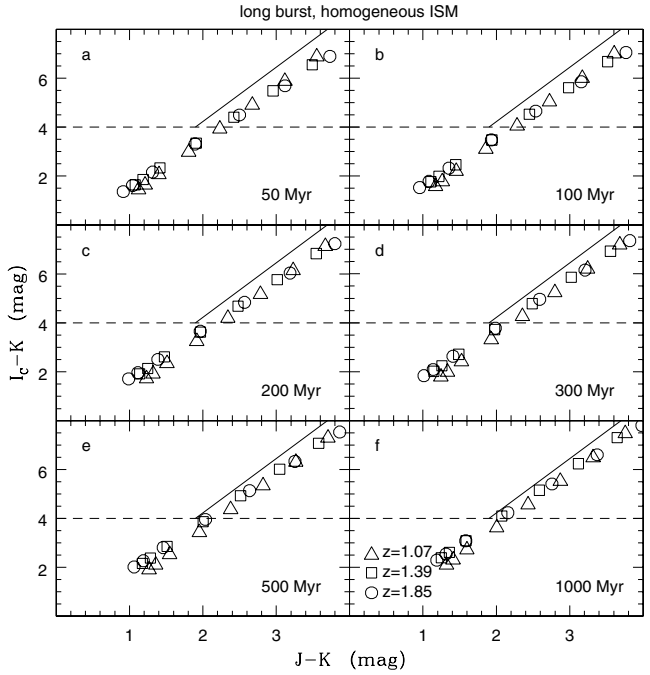

Figure 11. The same as in Fig. 10 but for a homogeneous dust distribution. Each panel shows models of selected age at different z, with τ_V increasing from 0.25 to 8 from the lower left to the upper right. DSGs with a 1-Gyr burst and a homogeneous dusty medium meet the PM00 classification criterion for ERGs. These DSGs may be bright enough to be selected as EROs (cf. Table 1).

Hence we confirm that there is a neat separation between passively evolving, old stellar populations (in a dust-free environment) and stellar populations formed in a continuous way in a dusty starburst, both at $1 < z < 2$ (PM00), which holds whatever the structure of the dusty medium and the amount of dust in the DSGs.

We do not explicitly consider the case of early, dusty post-starburst phases of a DSG with a long burst since the results obtained for basic model DPSGs in Section 4.2.1 qualitatively apply to this case. In particular, one may expect that this new class of DPSGs presents 'intruders' that have a lower amount of dust than 'intruder' basic model DPSGs observed at the same time after the end of the burst and at the same redshift, owing to the existence of the age/opacity degeneracy. This is indeed what we find. As an example, a 1.2-Gyr old dusty post-starburst phase following a burst with constant SFR $= 10^2$ M$_\odot$ yr^{-1} on a time-scale of 1 Gyr and observed at $z = 1.39$ has $I_c - K = 4.44$ (5.10) and $J - K = 1.95$ (2.31), if its clumpy dusty medium has $\tau_V = 2$ (20). This object falls well within the E domain (PM00) for $\tau_V = 2$ and, in general, is an 'intruder' for low/intermediate values of τ_V; it falls into the DSG domain (PM00) for high values of τ_V (e.g. 20 or less so). Conversely, a 0.3-Gyr old basic model DPSG observed at $z = 1.39$ is an 'intruder' when its clumpy dusty medium has $2 < \tau_V < 20$ (cf. Table 1).

4.3 The case of subsolar metallicities

From our further modelling and from the analysis of PM00 (their fig. 3c), it is easy to realize that the previous conclusions extend to Es and DSGs/DPSGs with metallicities different from the solar value. For example, we find 'intruders' among DPSGs with a two-phase clumpy distribution of the dust and a 1/10 solar metallicity (not shown). In this case, the 'intruders' are older than 300 Myr and have values of τ_V between 0.50 and 30 (according to their z).

4.4 The SED of an 'intruder' DPSG

Here we give an example of the non-negligible subsample of computed models of Es and DPSGs that populate the same region in the $I_c - K$ versus $J - K$ colour–colour plane (cf. Figs 7–9). Fig. 12 shows the normalized SED of an SSP (identified as a passively evolving elliptical galaxy) with Z$_\odot$ and age equal to 4 Gyr at $z = 1.39$ (thick solid line) and the normalized SED of a basic model DPSG with Z$_\odot$, age equal to 500 Myr and $\tau_V = 6$ at $z = 1.85$ (thin solid line). Each SED is in the observed frame and is normalized to the luminosity of the object at 2.17 μm. The spectral coverages of the I_c, J and K filters are shown as dashed areas. The visual inspection of Fig. 12 shows that these two objects have identical $I_c - K$ and $J - K$ colours. Indeed, $I_c - K = 5.01$ and $J - K = 2.11$ for the elliptical galaxy and $I_c - K = 4.97$ and $J - K = 2.09$ for the DPSG.[2]

In theory, complementary optical photometry in U, B and V may help distinguishing DPSGs at $1.3 < z < 2$ from Es at $1 < z < 2$, which cannot be distinguished by the PM00 classification criterion. Model Es have, for example, values of $V - R_c$ ranging from 2 to 3 when their $V - K$ ranges from 7.5 to 12, the former range being roughly 1 mag redder than that of model DPSGs with the same

[2] The elliptical galaxy has $K = 20.73$ (for a stellar mass of 7.5×10^{10} M$_\odot$), while the DPSG has $K = 21.04$. Hence these two models correspond to objects beyond the limiting K-band magnitude of the present ERO samples. N.B.: this is only a matter of normalization.

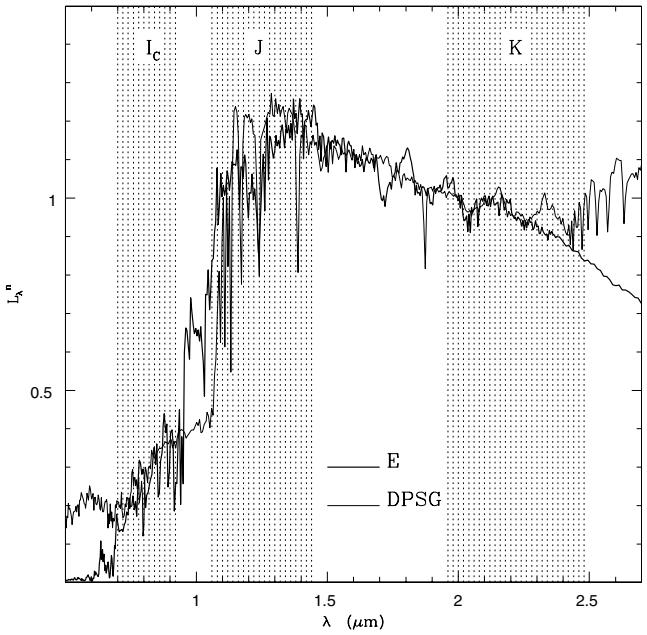

Figure 12. The SED of an SSP (i.e. an elliptical galaxy) with $Z_{\odot}$ and age of 4 Gyr at $z = 1.39$ (thick solid line) and the SED of a basic model DPSG with $Z_{\odot}$, age of 500 Myr and $\tau_V = 6$ at $z = 1.85$ (thin solid line). Each SED is in the observed frame and is normalized to the luminosity at 2.17 μm. The spectral coverages of the I_c, J and K filters are shown as dashed areas. It is evident that these two objects have similar $I_c - K$ and $J - K$ colours.

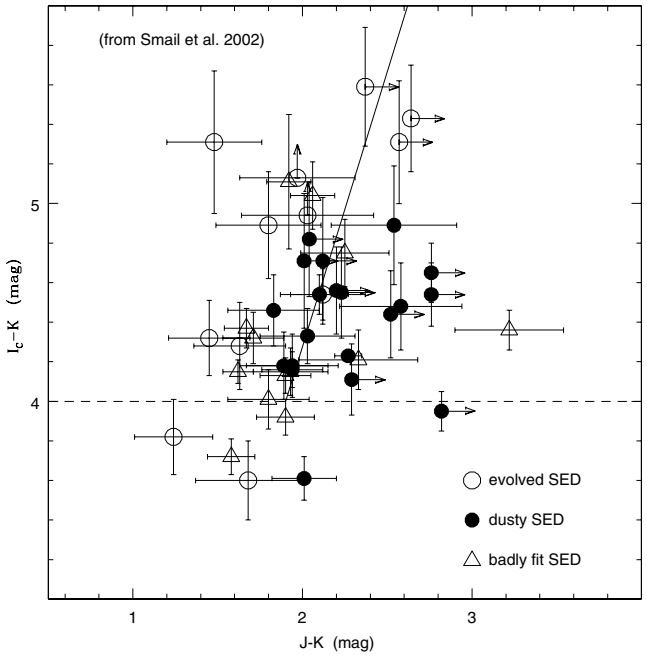

Figure 13. The distribution of 45 ERGs observed by Smail et al. (2002) in the $I_c - K$ versus $J - K$ colour–colour plane. ERGs classified by Smail et al. as evolved, dusty or other are reproduced as empty circles, filled circles and empty triangles, respectively. The short-dashed and solid lines represent the ERO selection function and the PM00 classification criterion for ERGs, respectively. Note that these objects were identified as EROs by Smail et al. on the basis of their $R_c - K$ colour.

$V - K$ colour. However, our models of the oldest Es and of the oldest, dustiest DPSGs, both at $1 < z < 2$, predict apparent magnitudes fainter than 28 V-mag, so that only the brightest ($21 < V < 26$) among these objects (either non-extremely attenuated DPSGs at $1 < z < 2$ or very massive Es at $z \sim 1$), seem to be easily detectable, given the current observational capabilities.

Hence we conclude and confirm that well-sampled SEDs are needed for a robust classification of ERGs (e.g. Smith et al. 2001; Miyazaki et al. 2002; Smail et al. 2002), and observations in X-rays, radio and/or far-IR/submillimetre (see the introduction). Photometry in the far-IR/submillimetre is suggested almost by default, even though present observational campaigns with SCUBA (Andreani et al. 1999; Mohan et al. 2002) show that the bulk of bright ($K <$ 19.5–20) ERGs have total mid-IR–millimetre rest-frame luminosities lower than those of ULIRGs. We discuss this in Section 5.

Finally, a way of distinguishing DPSGs from Es, both at high z, may be provided by the presence/absence of intermediate-age (i.e. 10^8–10^9 yr old) stellar populations. We will discuss this in a future paper.

4.5 On the classification of ERGs

The existence of dusty ERGs mixed with dust-free objects having passively evolving, old stellar populations (i.e. Es) and vice versa has been claimed recently by Miyazaki et al. (2002), following the application of the photometric redshift technique to multiwavelength photometry obtained for 247 EROs (see fig. 5 in their paper). Evidence in favour of the diversity of ERGs also comes from the multiwavelength analysis of 68 EROs by Smail et al. (2002) via a similar photometric redshift technique. Nevertheless, these authors conclude that the PM00 classification criterion is reasonably effective, at least in the $R_c - K$ versus $J - K$ colour–colour plane (see fig. 5 in Smail et al.).

Fig. 13 reproduces the distribution in the $I_c - K$ versus $J - K$ colour–colour plane of 45 ERGs out of the ERO sample of the previous authors. This subsample comprises ERGs brighter than $K =$ 20.5 (5σ) and detected at least in the I_c or J band. ERGs classified by Smail et al. as evolved (i.e. with passively evolving, old stellar populations in a dust-free environment), dusty (i.e. starburst) or other (i.e. with SEDs not matching those of the previous two classes) are reproduced as empty circles, filled circles and empty triangles, respectively. The visual inspection of Fig. 13 shows the following.

(i) Half of the dusty objects fall within 1σ of the PM00 separation line (on both sides). The existence of potential confusion near this separation line was stressed by PM00.

(ii) Two objects out of the 12 ERGs classified by Smail et al. as galaxies with evolved SEDs fall within 1σ from the PM00 separation line (on both sides).

(iii) Two more ERGs with evolved SEDs fall on the right-hand side of the PM00 separation line. They could be evolved galaxies at $z > 2$ (see PM00).

(iv) ERGs with SEDs more complex than evolved- or dusty-type fall everywhere.

For passively evolving, old ellipticals and dusty starbursts at $1 < z < 2$, the PM00 classification criterion, confirmed by our models (see Sections 4.1, 4.2 and 4.3), is statistically effective, as pointed out by Smail et al. (2002). Indeed, the median colours of these two galaxy populations are also separate (see table 2 in Smail et al.).

The more complex distribution in Fig. 13 (see also Miyazaki et al. 2002) is only partly accounted for by our theoretical exploration. In fact, we find that model DPSGs may overlap with model Es,

independent of their dust distribution (Section 4.2.1) and metallicity (Section 4.3).

Peculiar systems (e.g. AGN-host galaxies, mergers) or bulge+disc galaxies (with different composite stellar populations, affected by dust in different ways) at $1 < z < 2$ may also be part of the ERO population. In fact, the latter objects have been found by Smith et al. (2002), Miyazaki et al. (2002) and Yan & Thompson (2003).

The set of models discussed here does not account for these dusty galaxies. However, we note that a passively evolving, old, dust-free population associated with the bulge component of a bulge+disc galaxy may present redder colours than the same population associated with a dust-free elliptical galaxy, owing to the attenuation from the dust in the disc. At the same time, the disc stellar population may behave like a continuously star-forming, dusty galaxy with low/intermediate SFRs (cf. PM00). Hence a bulge+disc galaxy at $1 < z < 2$ may be expected to fall on both sides of the PM00 delimiting line. We defer to a future paper the investigation of normal bulge+disc galaxies at $z \geqslant 1$ as candidate ERGs.

4.6 On the photometric definition of EROs

Fig. 13 shows that three objects (with different classifications), selected as EROs by Smail et al. (2002) on the basis of their $R_c - K$ colour, do not match the $I_c - K$ colour selection criterion of EROs at more than 1σ, as already noted by these authors. Smail et al. find that their field contains 68 EROs with $R_c - K \geqslant 5.3$ against 99 objects with $I_c - K \geqslant 4$ and suggest that the latter is a less stringent definition of an unusually red source. In fact, 63 (93 per cent) of these 68 $R_c - K$ colour-selected EROs have $I_c - K \geqslant 4$.

With our models, we can investigate the nature of these 'ambiguous' objects. We find that model Es at $1 < z < 2$, brighter than $K = 20.5$, obey both the $R_c - K \geqslant 5.3$ and $I_c - K \geqslant 4$ colour selection criteria for EROs, whether dusty or not, for both solar and half-solar metallicities (not shown). Conversely, model DSGs/DPSGs at $1 < z < 2$, brighter than $K = 20.5$, selected via either $I_c - K$ or $R_c - K$, produce synthetic ERO samples with different objects and sizes, for both solar and a 1/10 solar metallicities. This is shown in Figs 14 and 15 for $Z_\odot$ DSGs with a short burst and DPSGs, both with a two-phase clumpy dust distribution, and for $Z_\odot$ DSGs with a long burst and a homogeneous dust distribution, respectively.

Interestingly, the $R_c - K \geqslant 5.3$ colour selection criterion systematically excludes more basic model DSGs/DPSGs at $1.3 < z < 2$ (mostly 300-Myr old DPSGs with $0.50 \leqslant \tau_V \leqslant 10$, but also DSGs with $\tau_V = 40$). Conversely, the $I_c - K \geqslant 4$ colour selection criterion tends to exclude more DSGs/DPSGs at $z \sim 1$ (mostly 500-Myr old DPSGs, with $4 \leqslant \tau_V \leqslant 20$). In the case of model DSGs with a short burst and DPSGs with a homogeneous dust distribution, the $R_c - K \geqslant 5.3$ colour selection criterion systematically excludes 300-Myr old DPSGs with $\tau_V = 1$ and 500-Myr old DPSGs with $\tau_V = 0.50$, both at $z > 1.8$. Conversely, there is no evidence for a bias in z, caused by the different colour selection criteria, for model DSGs with a long burst, whatever the structure of the dusty medium is (not shown). However, these DSGs are excluded by the $R_c - K \geqslant 5.3$ colour selection criterion if they have $\tau_V = 30$ (two-phase clumpy case) or $2 \leqslant \tau_V \leqslant 3$ (homogeneous case). Thus we conclude that selection via the $R_c - K$ colour biases the resultant ERO sample towards a larger ratio of Es (at any z between 1 and 2) to DSGs/DPSGs at $1.3 < z < 2$; vice versa, selection via the $I_c - K$ colour biases it towards a larger ratio of Es (at any z between 1 and 2) to DSGs/DPSGs at $z \sim 1$.

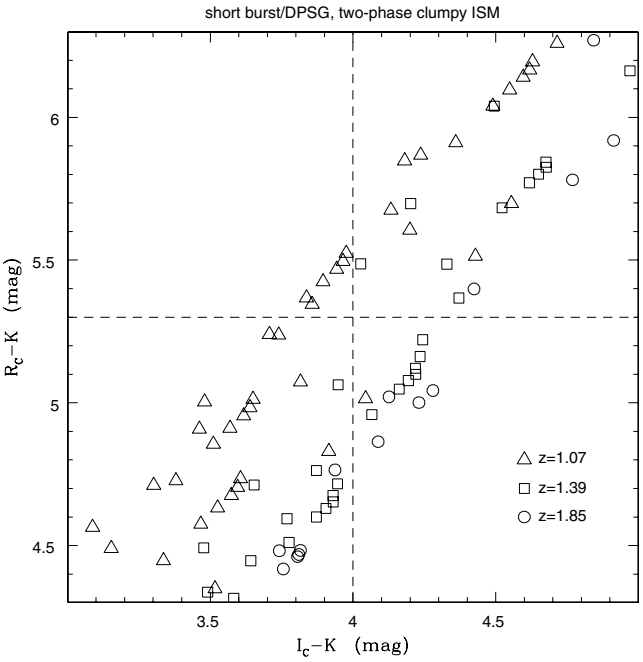

Figure 14. The distribution in the $R_c - K$ versus $I_c - K$ colour–colour plane of dusty stellar systems formed in a short burst, of $Z_\odot$ and different ages, at $1 < z < 2$, brighter than $K = 20.5$ and with a two-phase clumpy dust distribution. The two short-dashed lines represent the $R_c - K \geqslant 5.3$ and $I_c - K \geqslant 4$ selection functions of EROs. ERO selection via either colour criterion produces samples with different objects and sizes. A selection effect in z is present.

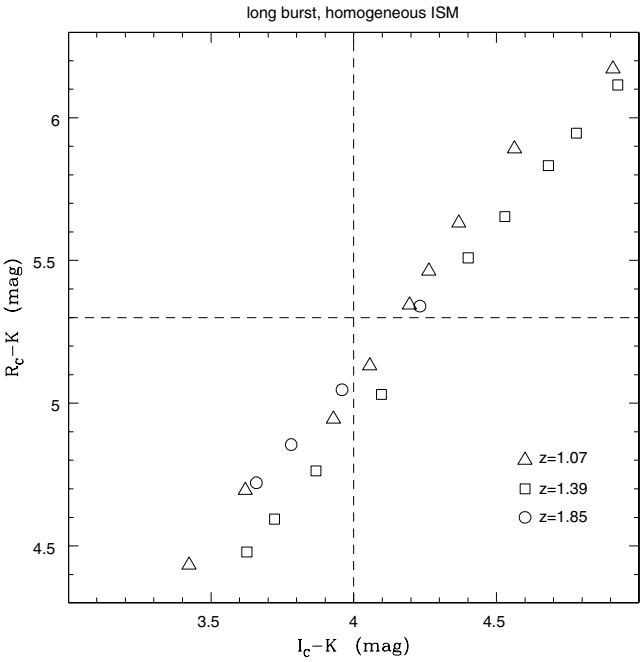

Figure 15. The distribution in the $R_c - K$ versus $I_c - K$ colour–colour plane of model DSG with a long burst, of $Z_\odot$ and different ages, at $1 < z < 2$, brighter than $K = 20.5$ and with a homogeneous dust distribution. Conclusions are the same as in Fig. 14, but for the absence of a selection effect in z.

In addition, we find that ERO selection via the $R_c - K$ colour tends to exclude DSGs/DPSGs brighter than $K = 20.5$ at $1.3 < z < 2$, if they have relatively low amounts of dust (i.e. with $0.50 \leqslant \tau_V \leqslant 3$), whatever the structure of the dusty medium.

Hence large discrepancies may be expected in the total number of selected EROs and in the statistical properties of the different subpopulations of ERGs present in a given ERO sample, whether selection is via $R_c - K$ or $I_c - K$. These considerations help us to understand the 33 per cent mismatch in the number of EROs selected via either $R_c - K$ or $I_c - K$ found by Smail et al. (2002).

We note that Yan & Thompson (2003) conclude that the Es-to-DSGs ratio in a given ERO sample is larger, when selection is via the $R_c - K$ colour instead of the $I_c - K$ colour, on the basis of the observed optical/near-IR colours expected for model stellar populations (Bruzual & Charlot[3]) approximating a passively evolving, old elliptical or simulating galaxies of different ages with extended star formation activity, all at $z \sim 1$. However, they do not consider dust attenuation. Our results support and complement their conclusion.

5 TOTAL MID-IR–(SUB)MILLIMETRE EMISSION OF DUSTY STARBURST/POST-STARBURST GALAXIES AT $1 < Z < 2$

Here we detail the relation between the amount of dust and the structure of the dusty medium, on one hand, and total mid-IR–(sub)millimetre emission from dust, on the other hand, for model DSGs/DPSGs. The radiative transfer models described in Section 2.2.2 do not model re-emission from dust, and, thus, we cannot produce and analyse SEDs in the rest-frame mid-IR–(sub)millimetre for these stellar systems. However, they provide a robust estimate of the total emission of model DSGs/DPSGs at these wavelengths, as given by the amount of light absorbed by internal dust in the wavelength range 0.1–3 μm (in the rest frame). We refer to this estimate as $L_{\rm dust}$.

We find that $L_{\rm dust}$ has a dynamic range of more than 500 (from $\sim 10^{10}$ to $\sim 5.6 \times 10^{12}$ $L_\odot$) for DPSGs to DSGs, as a function of the dust parameter space. In particular, $L_{\rm dust}$ ranges between 2 and 5.6×10^{12} $L_\odot$ for DSGs with a short burst, between 2 and 7.6×10^{11} $L_\odot$ for DSGs with a long burst, and between 10^{10} and 5.7×10^{11} $L_\odot$ for DPSGs. For fixed dust parameters, $L_{\rm dust}$ increases (up to 50 per cent) with increasing age for both DSGs, but decreases (down to an order of magnitude) with increasing age for DPSGs. Conversely, for a fixed age, $L_{\rm dust}$ increases by a factor of approximately 3 when τ_V increases from 0.25 to 50 (from 0.25 to 8) for the two-phase clumpy (homogeneous) case, for both DSGs and DPSGs.

The reason for the high dynamic range in $L_{\rm dust}$ is twofold. On one hand, a dusty medium with given dust type absorbs stellar light at a given wavelength with an efficiency that depends strongly on the amount of dust, the structure of the dusty medium and the distribution of this medium with respect to the stellar sources. Hence all these aspects contribute to determining the re-emission from dust grains in the mid-IR–(sub)millimetre wavelength domain. This is investigated in details by Misselt et al. (2001) for the same dust/stars geometry of a DSG/DPSG as that assumed in Section 2.2.2. Here it is important to stress that model DSGs/DPSGs selected as ERGs have very different dust properties (cf. Table 1).[4]

On the other hand, dust absorbs and scatters UV photons more efficiently than optical/near-IR ones. Available optical/near-IR photons may replace available UV photons as the major source of dust heating, if the optical depth at optical/near-IR wavelengths of the dusty medium is large enough. For a model DPSG, the intrinsic UV-to-optical luminosity ratio decreases towards 0 when the model age approaches 1 Gyr (Fig. 1). Thus ageing DPSGs will tend to have lower and lower total mid-IR–(sub)millimetre luminosities, for fixed dust parameters.

For the dust parameter space explored here, only model DSGs with SFR $= 10^3$ $M_\odot$ yr^{-1} over a time-scale of 100 Myr may be associated with $L_{\rm dust} \geqslant 10^{12}$ $L_\odot$ and, thus, be classified as ULIRGs. Conversely, model DSGs with SFR $= 10^2$ $M_\odot$ yr^{-1} over a time-scale of 1 Gyr typically have total mid-IR–(sub)millimetre luminosities of a few to several $\times 10^{11}$ $L_\odot$. DPSGs may be associated with even lower values of dust emission (down to $\sim 10^{10}$ $L_\odot$), especially when the post-burst stellar population approaches 1 Gyr. Hence we conclude that the bulk of model DSGs/DPSGs does not belong to the ULIRG class. This is true also for model DSGs/DPSGs selected as EROs with $K < 20.5$ (cf. Table 1).

Our conclusion is consistent with those of Andreani et al. (1999) and Mohan et al. (2002), which are based on observational results for a slightly brighter ERO sample (see the introduction).

6 DISCUSSION AND CONCLUSIONS

In the previous sections we have modelled the spectral energy distributions of simple stellar populations, intended to simulate passively evolving, old ($\geqslant$1 Gyr) elliptical galaxies and the SEDs of young ($\leqslant$0.1 Gyr)/intermediate-age (0.1–1 Gyr), dusty starburst galaxies and of intermediate-age, dusty post-starburst galaxies, all at $1 < z < 2$, as candidate (EROs).

In the early post-starburst phases, massive stars are absent (owing to the absence of star formation) but intermediate-age stars are present. For these phases, we assume that at least part of the dusty medium of the previous starburst phase survives during a maximal time window of 0.9 Gyr.

We have investigated observed optical/near-IR colours and magnitudes of the previous models and, in particular, the distribution in the $I_c - K$ versus $J - K$ colour–colour plane. In this colour–colour diagram, Pozzetti & Mannucci (2000) claim that passively evolving, old stellar populations in a dust-free environment (i.e. elliptical galaxies) and stellar populations produced continuously in a dusty starburst galaxy are reasonably well separated, whatever the dust/stars configuration.

This study complements the seminal analysis of Pozzetti & Mannucci for four main reasons.

(i) We make the new case of *dusty post-starburst galaxies* at $1 < z < 2$ as candidate EROs. In particular, we discuss the early, dusty post-starburst phases of stellar systems formed (mostly) at $1 < z < 2$, in a single burst of finite duration ($t_{\rm burst}$) of the order of 0.1 Gyr (short burst). The results obtained for these DPSGs may be easily extended to coeval, early, dusty post-starburst phases of galaxy formation in a single burst with, for example, $t_{\rm burst} = 1$ Gyr (long burst), when the existence of a degeneracy between age and opacity of the models (Takagi et al. 1999) is taken into account.

We note that the DSGs with long or short bursts under investigation sustain star formation rates of the order of 10^2 or 10^3 $M_\odot$ yr^{-1},

[3] See ftp://gemini.tuc.noao.edu/pub/charlot/bca5

[4] In particular, we note that structure of the dusty medium may be traded for the amount of dust in producing a given value of $L_{\rm dust}$. This is a caveat against the simplistic use of dust emission as a proxy for the amount of dust in dusty ERGs.

respectively. SFRs $\sim 10^3$ $M_\odot$ yr^{-1} have been inferred from observations of high-z (sub)millimetre sources (e.g. Smail et al. 1997, 2003; Barger et al. 1998; Cimatti et al. 1998; Hughes et al. 1998; Eales et al. 1999; Bertoldi et al. 2000; Lutz et al. 2001).

The presence of a considerable population of starburst galaxies with large SFRs over a short ($\sim$100 Myr) time-scale at $1 < z < 2$ is qualitatively consistent with the interpretation of the Lick absorption-line indices of nearby intermediate-mass (i.e. with a velocity dispersion of $\sim$200 km s^{-1}) early-type galaxies by Thomas et al. (2002).

(ii) We explore the impact of dust attenuation (Witt et al. 1992) on the optical/near-IR colours of dusty Es at $1 < z < 2$.

(iii) For all DSGs/DPSGs, we adopt a new dust/stars geometry (Witt & Gordon 2000) and explore the impact of dust distribution (two-phase clumpy versus homogeneous) and amount of dust on the observed optical/near-IR colours. This geometry is consistent with observed properties of nearby starbursts (Gordon et al. 1997) and Lyman-break galaxies at $2 < z < 4$ (Vijh et al. 2003).

(iv) We calculate the total emission from dust in the rest-frame mid-IR–(sub)millimetre for DSGs/DPSGs.

The distribution of model Es and DSGs/DPSGs at $1 < z < 2$ in the optical/near-IR colour–magnitude and colour–colour diagrams reproduces well that of observed extremely red galaxies (Sections 3 and 4). Hereafter we summarize our results.

(i) We find that DPSGs, with ages between 0.2 and 1 Gyr, at $1.3 < z < 2$ may mix with Es at $1 < z < 2$ in the $I_c - K$ versus $J - K$ colour–colour diagram, for a large range in the amount of dust. This holds whatever the structure (two-phase clumpy or homogeneous) of the dusty medium. This result is a source of concern for the two-colour classification criterion of Pozzetti & Mannucci. (2000)

(ii) Conversely, intermediate-age DPSGs at $z \sim 1$ may mix with DSGs of age less than 1 Gyr at $1 < z < 2$ in the same colour–colour plot, for a large range in the amount of dust and whatever the structure of the dusty medium. This result and the previous one could explain in part the complexity of the ERG classification recently emerged from the analysis of statistical samples of EROs, where this classification was based on multiwavelength photometry (e.g. Miyazaki et al. 2002; Smail et al. 2002) and not on optical/near-IR colour–colour plots.

(iii) On the other hand, we confirm the result of Pozzetti & Mannucci (2000). In addition, we find that this result holds whether the dusty medium of a DSG is two-phase clumpy or homogeneous and whether high-z ellipticals are dust-free or as dusty as nearby ones.

(iv) Model Es at $1 < z < 2$ populate a narrow locus in the $I_c - K$ versus $J - K$ colour–colour plane, whether dusty or not. This means that dust attenuation may explain very red $I_c - K$ and $J - K$ colours for ellipticals at $1 < z < 2$ without the need to invoke extremely old ages and/or higher metallicities and/or higher redshifts.

(v) The picture is the same when the distribution of the models in the $R_c - K$ versus $J - K$ colour–colour plane is investigated (cf. Pozzetti & Mannucci 2000). Hence we conclude and confirm that well-sampled SEDs are needed for a robust classification of ERGs (e.g. Smith et al. 2001; Miyazaki et al. 2002; Smail et al. 2002), and observations in X-rays (Alexander et al. 2002; Brusa et al. 2002; Smail et al. 2002, but see Stevens et al. 2003), radio (Smail et al. 2002) and/or far-IR/submillimetre (Cimatti et al. 1998; Andreani et al. 1999; Mohan et al. 2002).

(vi) We find that the total rest-frame mid-IR–(sub)millimetre luminosity ranges from $\sim 10^{10}$ to $\sim 5.6 \times 10^{12}$ $L_\odot$ for DPSGs to DSGs. This high dynamic range is consistent with the large range in total rest-frame mid-IR–(sub)millimetre luminosity estimated for ERGs observed in the submillimetre range (Cimatti et al. 1998; Andreani et al. 1999; Mohan et al. 2002).

This study offers two viable, not mutually exclusive interpretations to the observational results and conclusions of the previous authors. One interpretation is that re-emission by dust grains in the mid-IR–(sub)millimetre wavelength domain depends on dust type and amount, structure of the dusty medium and dust/stars configuration, since the absorption efficiency of stellar light at given wavelength depends on these parameters. We find that the extremely red colours of DSGs/DPSGs at $1 < z < 2$ do not necessarily indicate large amounts of dust (Section 3), as instead believed for SCUBA submillimetre sources, for example, and may be reproduced over a very large range in structure of the dusty medium. Hence the submillimetre fluxes of DSGs/DPSGs at $1 < z < 2$ are not expected to be necessarily similar to those of SCUBA submillimetre sources at similar/higher z.

The other interpretation is the reduced contribution of UV photons to dust heating in the model DPSGs, which seem to constitute a non-negligible, candidate ERO subpopulation. Dust absorbs and scatters more efficiently UV photons than optical/near-IR ones. Available optical/near-IR photons may replace available UV photons as the major source of dust heating if the optical depth at optical/near-IR wavelengths of the dusty medium is large enough. For a model DPSG, the intrinsic UV-to-optical luminosity ratio decreases towards 0 when its age approaches 1 Gyr (Fig. 1). Thus ageing DPSGs will tend to have lower and lower total rest-frame mid-IR–(sub)millimetre luminosities, for fixed dust parameters.

(vii) Furthermore, for the dust-parameter space considered here, we find that only model DSGs with SFR $= 10^3$ $M_\odot$ yr^{-1} over a time-scale of 100 Myr may be associated with a total mid-IR–(sub)millimetre luminosity (in the rest frame) greater than 10^{12} $L_\odot$ and, thus, be classified as ULIRGs. Conversely, model DSGs with SFR $= 10^2$ $M_\odot$ yr^{-1} over a time-scale of 1 Gyr typically have total mid-IR–(sub)millimetre luminosities of a few to several $\times 10^{11}$ $L_\odot$. DPSGs may be associated with even lower values of dust emission (down to $\sim 10^{10}$ $L_\odot$). We conclude that the bulk of dusty, bright ($K < 20.5$) ERGs are not associated with ULIRGs, consistent with the conclusion of Andreani et al. (1999) and Mohan et al. (2002), based on observations of a slightly brighter sample.

(viii) Typical ground-based surveys with $K < 20.5$ (e.g. Drory et al. 2001; Cimatti et al. 2002b; Smail et al. 2002) are biased against the following objects at $1 < z < 2$ (if any): ellipticals (dusty or not) with stellar masses lower than $\sim 10^{11}$ $M_\odot$; dusty starbursts with, for example, a constant SFR $\leqslant 10^2$ $M_\odot$ yr^{-1} (10 $M_\odot$ yr^{-1}) on a time-scale of 0.1 (1) Gyr, identified as events of low-mass galaxy formation at these redshifts; early, dusty post-starburst phases of these dusty starbursts.

(ix) Model Es (whether dusty or not) at $1 < z < 2$ are always selected as EROs (if massive enough), whether selection is via the $I_c - K$ or $R_c - K$ colour.

(x) Conversely, selection of observable (i.e. with $K < 20.5$), coeval DSGs/DPSGs as EROs is a complex function of the properties of their dusty medium. The explanation is that the extremely red colours ($R_c - K \geqslant 5.3$ or $I_c - K \geqslant 4$) of model DSGs/DPSGs at $1 < z < 2$ derive from radiative transfer through their dusty media.

(xi) We find that selection via the $R_c - K$ colour biases the resultant sample of observable EROs towards a larger ratio of Es (at any z between 1 and 2) to DSGs/DPSGs at $1.3 < z < 2$; vice versa, selection via the $I_c - K$ colour bias it towards a larger ratio of Es (at any z between 1 and 2) to DSGs/DPSGs at $z \sim 1$. This result confirms and complements that of Yan & Thompson (2003).

Hence important discrepancies may be expected in the total number of selected EROs and in the statistical properties of the different subpopulations of ERGs present in a given ERO sample, whether selection is via $R_c - K$ or $I_c - K$. For example, DSGs/DPSGs at $1.3 < z < 2$ with the lowest amount of dust are not selected as EROs via the $R_c - K \geqslant 5.3$ colour criterion.

These considerations help us to understand the 33 per cent mismatch in the number of EROs with $K < 20.5$ selected via either $R_c - K$ or $I_c - K$ found by Smail et al. (2002).

ACKNOWLEDGMENTS

We acknowledge the anonymous referee, who contributed to the improvement of this paper in its final version with her/his stimulating, insightful comments and suggestions.

REFERENCES

Adelberger K.L., Steidel C.C., Shapley A.E., Pettini M., 2003, ApJ, 584, 45
Alexander D.M., Vignali C., Bauer F.E., Brandt W.N., Hornschemeier A.E., Garmire G.P., Schneider D.P., 2002, AJ, 123, 1149
Andreani P., Cimatti A., Röttgering H., Tilanus R., 1999, Ap&SS, 266, 267
Barger A.J., Cowie L.L., Sanders D.B., Fulton E., Taniguchi Y., Sato Y., Kawara K., Okuda H. , 1998, Nat, 394, 248
Barsella B., Ferrini F., Greenberg J.M., Aiello S., 1989, A&A, 209, 349
Beck R., Carilli C.L., Holdaway M.A., Klein U., 1994, A&A, 292, 409
Bertoldi F. et al., 2000, A&A, 360, 92
Bessel M.S., Brett J.M., 1988, PASP, 100, 1134
Bianchi S., Ferrara A., Giovanardi C., 1996, ApJ, 465, 127
Branch D., Livio M., Yungelson L.R., Boffi F.R., Baron E., 1995, PASP, 107, 1019
Brusa M., Comastri A., Daddi E., Cimatti A., Mignoli M., Pozzetti L., 2002, ApJ, 581, L89
Calzetti D., 1997, AJ, 113, 162
Calzetti D., Kinney A.L., Storchi-Bergmann T., 1994, ApJ, 429, 582
Calzetti D., Armus L., Bohlin R.C., Kinney A.L., Koornneef J., Storchi-Bergmann T., 2000, ApJ, 533, 682
Cimatti A., Bianchi S., Ferrara A., Giovanardi C., 1997, MNRAS, 290, L43
Cimatti A., Andreani P., Röttgering H., Tilanus R., 1998, Nat, 392, 895
Cimatti A. et al., 1999, A&A, 352, L45
Cimatti A. et al., 2002a, A&A, 381, L68
Cimatti A. et al., 2002b, A&A, 392, 395
Cousins A.W.J., 1976, MNRAS, 81, 25
Davies J.I., Alton P.B., Bianchi S., Trewhella M., 1998, MNRAS, 300, 1006
Drory N., Feulner G., Bender R., Botzler C. S., Hopp U., Maraston C., Mendes de Oliveira C., Snigula J., 2001, MNRAS, 325, 550
Dwek E. et al., 1983, ApJ, 274, 168
Eales S., Lilly S., Gear W., Dunne L., Bond J.R., Hammer F., Le Févre O., Crampton D., 1999, ApJ, 515, 518
Elbaz D., Flores H., Chanial P., Mirabel I.F., Sanders D., Duc P.-A., Cesarsky C.J., Aussel H., 2002, A&A, 381, L1
Ellison D.C., Drury L. O'C., Meyer J.-P., 1997, ApJ, 487, 197
Elston R., Rieke G.H., Rieke M.J., 1988, ApJ, 331, L77
Fanelli M.N., O'Connell R.W., Thuan T.X., 1988, ApJ, 334, 665
Fioc M., Rocca-Volmerange B., 1997, A&A, 326, 950
Gavazzi G., Pierini D., Boselli A., 1996, A&A, 312, 397
Gehrz R., 1989, in Allamandola L.J., Tielens A.G.G.M., eds, Proc. IAU Symp. 135, Interstellar Dust. Kluwer, Dordrecht, p. 445
Gordon K.D., Calzetti D., Witt A.N., 1997, ApJ, 487, 625 (GCW97)
Granato G.L., Silva L., Monaco P., Panuzzo P., Salucci P., De Zotti G., Danese L., 2001, MNRAS, 324, 757
Greenberg J.M., Ferrini F., Barsella B., Aiello S., 1987, Nat, 327, 214
Heckman T.M., 2001, in Hibbard J.E., Rupen M., van Gorkom J.H., eds, Proc. ASP Conf. 240, Gas and Galaxy Evolution. Astron. Soc. Pac., San Francisco, p. 345
Hirashita H., Ferrara A., 2002, MNRAS, 337, 921
Hirashita H., Hunt L.K., Ferrara A., 2002, MNRAS, 330, L19
Hughes D.H. et al., 1998, Nat, 394, 241
Jones A.P., Tielens A.G.G.M., Hollenbach D.J., 1996, ApJ, 469, 740
Kauffmann G., Charlot S., White S.D.M., 1996, MNRAS, 283, 117
Kozasa T., Hasegawa H., Nomoto K., 1991, A&A, 249, 474
Lutz D. et al., 2001, A&A, 378, 70
McKee G., 1989, in Allamandola L.J., Tielens A.G.G.M., eds, Proc. IAU Symp. 135, Interstellar Dust. Kluwer, Dordrecht, p. 431
Mannucci F., Pozzetti L., Thompson D., Oliva, E., Baffa C., Comoretto G., Gennari S., Lisi F., 2002, MNRAS, 329, L57
Maraston C., 1998, MNRAS, 300, 872
Mas-Hesse J.M., Arnault P., Kunth D., 1989, Ap&SS, 157, 131
Misselt K.A., Gordon K.D., Clayton G.C., Wolff M.J., 2001, ApJ, 551, 277
Miyazaki M. et al., 2002, preprint astro-ph/0210509
Mohan N.R., Cimatti A., Roettgering H.J.A., Andreani P., Severgnini P., Tilanus R.P.J., Carilli C.L., Stanford S.A., 2002, A&A, 383, 440
Moriondo G., Cimatti A., Daddi E., 2000, A&A, 364, 26
Moseley S.H., Dwek E., Glaccum W., Graham J.R., Loewenstein R.F., 1989, Nat, 340, 697
Nakai N., Hayashi M., Handa T., Sofue Y., Hasegawa T., Sasaki M., 1987, PASJ, 39, 68
Norman C.A., Ferrara A., 1996, ApJ, 467, 280
Phillips A., 1993, AJ, 105, 486
Pozzetti L., Mannucci F., 2000, MNRAS, 317, L17 (PM00)
Saglia R.P., Maraston C., Greggio L., Bender R., Ziegler B., 2000, A&A, 360, 911
Salpeter E., 1955, ApJ, 121, 161
Shu C., Mo H.J., Mao S., 2003, preprint astro-ph/0301035
Smail I., Ivison R.J., Blain A.W., 1997, ApJ, 490, L5
Smail I., Owen F.N., Morrison G.E., Keel W.C., Ivison R.J., Ledlow M.J., 2002, ApJ, 581, 844
Smail I., Ivison R.J., Gilbank D.G., Dunlop J.S., Keel W.C., Motohara K., Stevens J.A., 2003, ApJ, 583, 551
Smith G.P., Treu T., Ellis R., Smail I., Kneib J.-P., Frye B.L., 2001, ApJ, 562, 635
Smith G.P., Smail I., Kneib J.-P., Davis C.J., Takamiya M., Ebeling H., Czoske O., 2002, MNRAS, 333, L16
Springel V., Hernquist L., 2003, MNRAS, 339, 312
Stevens J.A., Page M.J., Ivison R.J., Smail I., Lehmann I., Hasinger G., Szokoly G., 2003, MNRAS, 342, 249
Stiavelli M., Treu T., 2001, in Funes J.G., Corsini E.M., eds, Proc. ASP Conf. 230, Galaxy Disks and Disk Galaxies. Astron. Soc. Pac., San Francisco, p. 603
Suchkov A.A., Balsara D.S., Heckman T.M., Leitherer C., 1994, ApJ, 430, 511
Suchkov A.A., Berman V.G., Heckman T.M., Balsara D.S., 1996, ApJ, 463, 528
Takagi T., Arimoto N., Vansevicius V., 1999, ApJ, 523, 107
Takeuchi T.T., Hirashita H., Ishii T.T., Hunt L.K., Ferrara A., 2003, MNRAS, 343, 839
Thomas D., Maraston C., Bender R., 2002, Ap&SS, 281, 371
Todini P., Ferrara A., 2001, MNRAS, 325, 726
Totani T., Yoshii Y., Iwamuro F., Maihara T., Motohara K., 2001, ApJ, 558, L87
Vijh U., Gordon K.D., Witt A.N., 2003, ApJ, 587, 533
White S.S.M., Frenk C.S., 1991, ApJ, 379, 52
Wise M.W., Silva D.R., 1996, ApJ, 461, 155
Witt A.N., Gordon K.D., 2000, ApJ, 528, 799 (WG00)
Witt A.N., Thronson H.A., Capuano J.M., 1992, ApJ, 393, 611 (WTC92)
Yan L., Thompson D., 2003, ApJ, 586, 765

APPENDIX A: THE NON-IMPORTANCE OF THE NEBULAR CONTINUUM

We reproduce the distribution in the $I_c - K$ versus $J - K$ colour–colour plane of $Z_{\odot}$ DSGs with a short burst and DPSGs (Fig. A1) and DSGs with a long burst (Fig. A2), all of them with a

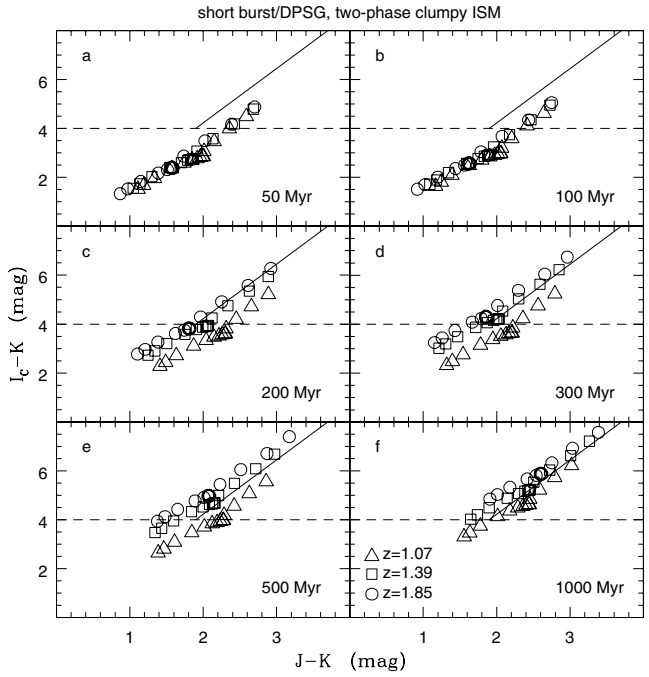

Figure A1. $I_c - K$ versus $J - K$ for $Z_\odot$ model DSGs with a short burst and DPSGs, all of them with a two-phase clumpy dusty medium, as a function of age and z, when no nebular emission is taken into account, and its attenuation from dust. In each panel τ_V increases from 0.25 to 50 from the lower left to the upper right. Lines and symbols are the same as in Fig. 8. Conclusions are the same as those reached from Fig. 8.

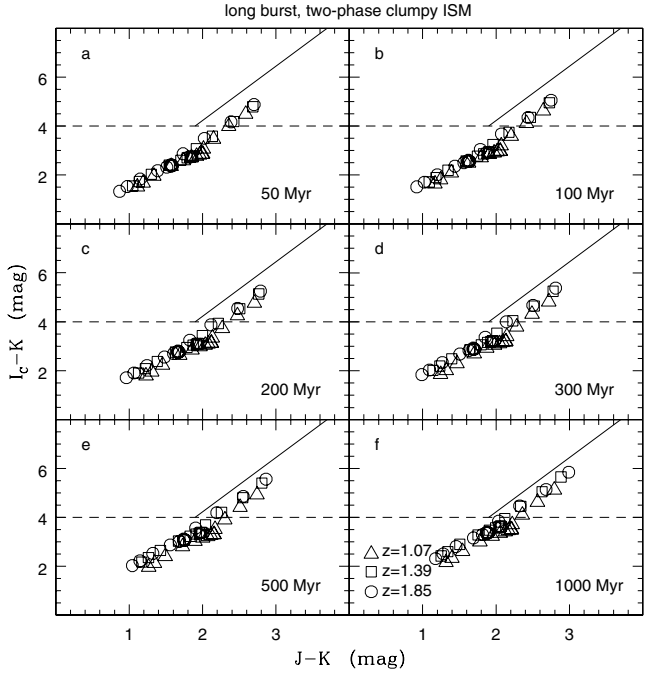

Figure A2. The same as in Fig. A1 but for DSGs with a long burst. In each panel τ_V increases from 0.25 to 50 from the lower left to the upper right. Conclusions are the same as those reached from Fig. 10.

two-phase clumpy dust distribution, as a function of age and redshift, when no nebular emission is computed. Hence no attenuation of the gas emission, either in the line or in the continuum, from dust is computed as well. Models are represented as in Figs 8 and 10, respectively, where nebular emission was taken into account together with its attenuation from dust as described in Section 2.2.2.

From the comparison of these four figures it emerges that nebular emission and its attenuation do not play a role in the selection of a DSG/DPSG at $1 < z < 2$ as an ERO. They do not affect the presence of 'intruder' DPSGs either. Hence we conclude that the main results of Section 4.2 do not depend on our choice of dust attenuation for the nebular emission.

APPENDIX B: ON THE APPLICATION OF THE CALZETTI LAW TO DUSTY ERGS

Calzetti et al. (1994) have empirically constrained an extinction function from the UV and optical spectra of 39 starburst and blue compact galaxies at $z = 0$. This extinction curve has an overall UV/optical slope flatter than the MW one and lacks the 2175-Å dust absorption feature, as confirmed by GCW97. Further inclusion of IR broad-band data for 19 of these 39 galaxies helped constrain the shape of the characteristic (i.e. *average*) attenuation function, but not fix its zero-point (Calzetti 1997). The absolute calibration of the attenuation function of DSG at $z = 0$ was possible owing to the availability of far-IR photometry for a subsample of only five objects (Calzetti et al. 2000). In its final layout, the so-called 'Calzetti law' has a fixed wavelength dependence (as shown in Fig. 2) and is normalized to the stellar-continuum reddening $E(B - V)_{\rm star}$. Since its discovery, the Calzetti law has been used to describe dust attenuation in DSGs at high z (e.g. Cimatti et al. 2002a) under the intrinsic assumption that dust properties and content, as well as dust/stars distribution and structure of the dusty medium, are similar in high-z DSGs and in the nearby starbursts of the Calzetti sample.

Thus we produce new models of $Z_\odot$ DSGs with a short burst and DPSGs (Fig. B1), and DSGs with a long burst (Fig. B2) by adopting the Calzetti law instead of the simulated attenuation curves described in Section 2.2.2. Two values of the stellar-continuum reddening (i.e. 0.5 and 0.8) are considered, as in PM00 and consistent with Cimatti et al. (2002a). Even in this case we find that model DPSGs partially 'intrude' into the region populated by passively evolving, old Es, if they are 'moderately attenuated' [i.e. $E(B - V)_{\rm star} = 0.5$] and at $1.3 < z < 2$ (Fig. B1). Conversely, among the model DSGs with a long burst and attenuated according to the Calzetti law, no 'intruders' are found (Fig. B2). Hence the main results of Section 4.2 are confirmed here.

There are no 'intruders' with $4 \leqslant I_c - K \leqslant 5$ in Fig. B1, as instead in Fig. 8, but this is easy to understand. The original values of the Balmer line-emission reddening $E(B - V)$ found by Calzetti et al. (1994) for their sample range between 0 and 0.93, so that $E(B - V)_{\rm star}$ ranges between 0 and 0.41 for this sample, if $E(B - V)_{\rm star} = (0.44 \pm 0.03)E(B - V)$ (Calzetti 1997). Hence the observed values of $E(B - V)_{\rm star}$ are lower than those considered by PM00 and here. The mean of these observed values is consistent with the value of $E(B - V)_{\rm star}$ predicted by the WG00 SHELL configuration with SMC-type dust distributed in a two-phase clumpy medium and $\tau_V = 1.5$ (Fig. 3), which reproduces the Calzetti law rather well (Fig. 2). In Fig. 8 the 'intruders' with $4 \leqslant I_c - K \leqslant 5$ have low/intermediate values of τ_V and, thus, $E(B - V)_{\rm star} \leqslant 0.3$, consistent with the values obtained for the Calzetti sample.

Values of $E(B - V)_{\rm star} \geqslant 0.5$ (e.g. in Cimatti et al. 2002a) require either an enormous amount of dust, in the two-phase clumpy case, or low amounts of dust and a homogeneous dusty medium, for the SHELL configuration (Fig. 3). In both cases the wavelength

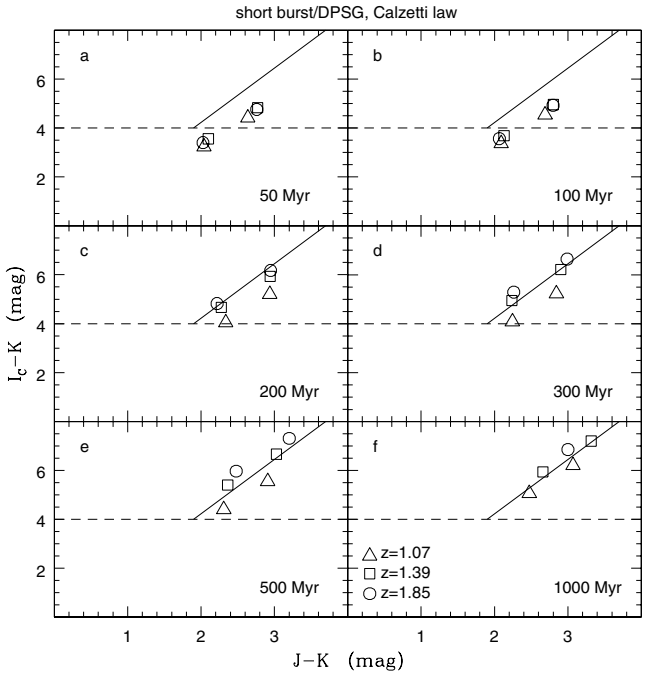

Figure B1. The distribution of $Z_{\odot}$ DSGs with a short burst and DPSGs in the $I_c - K$ versus $J - K$ colour–colour plane under the assumption that their attenuation function follows the Calzetti law. Lines are the same as in Fig. 8. Models of selected ages are reproduced with different symbols according to their redshift. DSGs/DPSGs with a stellar reddening $E(B-V)_{\rm star} = 0.5$ have bluer colours than those with $E(B-V)_{\rm star} = 0.8$. DPSGs attenuated with a Calzetti law 'intrude' into the region populated by passively evolving, old Es, consistent with the result of Section 4.2.1.

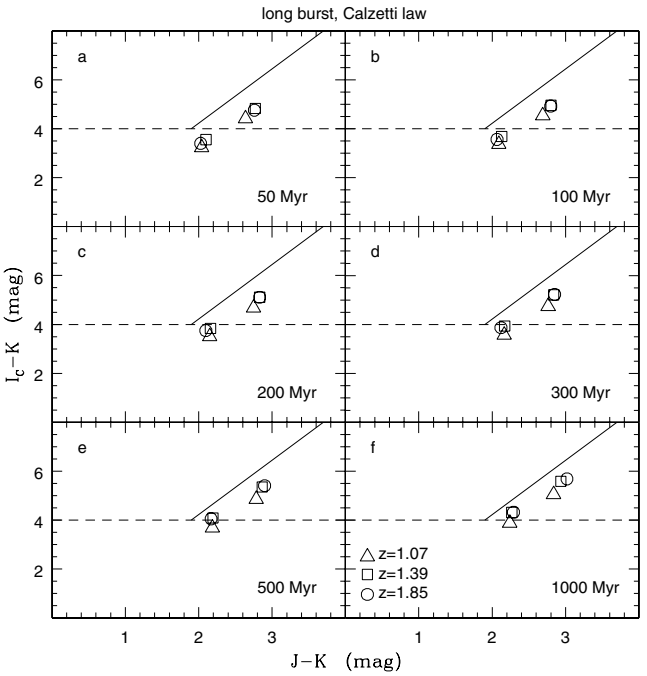

Figure B2. The same as in Fig. B1 but for $Z_{\odot}$ DSGs with a long burst. Models of selected ages are reproduced with different symbols according to their redshift. DSGs/DPSGs with a stellar reddening $E(B-V)_{\rm star} = 0.5$ have bluer colours than those with $E(B-V)_{\rm star} = 0.8$. In this case, no 'intruders' are found, consistent with the result of Section 4.2.2 and PM00.

dependence of the model attenuation function is quite different from the Calzetti law (Fig. 2). We conclude that the scaling of the functional form giving the wavelength dependence of the Calzetti law with arbitrary values of $E(B-V)_{\rm star} \geqslant 0.5$, under the assumption that reddening is a measure of dustiness, is not demonstrated from the observations and may be questionable on theoretical grounds (cf. Section 2.2.2), as also concluded by WG00.

This paper has been typeset from a TEX/LATEX file prepared by the author.